LEBANESE AMERICAN UNIVERSITY

Distinctive Role of StarD13 in Serous Ovarian Carcinoma Cell Proliferation, Metastasis, and Invadopodia Assembly

By

Sandra Abdullatef

A thesis submitted in partial fulfillment of the requirements for the degree of Master of Science in

Molecular Biology

School of Arts and Sciences

May 2019

LAU
الجامعة اللبنانية الأميركية
Lebanese American University

THESIS APPROVAL FORM

Student Name: Sandra Abdellatef I.D. #: 201206414

Thesis Title: the distinctive Role of starD13 in ovarian Cancer

Program: Msc. Molecular Biology

Department: Arts and science

School: Arts and science

The undersigned certify that they have examined the final electronic copy of this thesis and approved it in Partial Fulfillment of the requirements for the degree of:

Master's sc. in the major of Molecular Biology

Thesis Advisor's Name: Mirval El Sibai

Signature: [redacted] Date: 6 / 5 / 2019 (Day / Month / Year)

Committee Member's Name: Dr. Rayan Khalaf

Signature: [redacted] Date: 6 / 5 / 2019 (Day / Month / Year)

Committee Member's Name: Dr. Tarek Nawas

Signature: [redacted] Date: 6 / 5 / 2019 (Day / Month / Year)

LAU
الجامعة اللبنانية الأميركية
Lebanese American University

THESIS COPYRIGHT RELEASE FORM

LEBANESE AMERICAN UNIVERSITY NON-EXCLUSIVE DISTRIBUTION LICENSE

By signing and submitting this license, you (the author(s) or copyright owner) grants the Lebanese American University (LAU) the non-exclusive right to reproduce, translate (as defined below), and/or distribute your submission (including the abstract) worldwide in print and electronic formats and in any medium, including but not limited to audio or video. You agree that LAU may, without changing the content, translate the submission to any medium or format for the purpose of preservation. You also agree that LAU may keep more than one copy of this submission for purposes of security, backup and preservation. You represent that the submission is your original work, and that you have the right to grant the rights contained in this license. You also represent that your submission does not, to the best of your knowledge, infringe upon anyone's copyright. If the submission contains material for which you do not hold copyright, you represent that you have obtained the unrestricted permission of the copyright owner to grant LAU the rights required by this license, and that such third-party owned material is clearly identified and acknowledged within the text or content of the submission. IF THE SUBMISSION IS BASED UPON WORK THAT HAS BEEN SPONSORED OR SUPPORTED BY AN AGENCY OR ORGANIZATION OTHER THAN LAU, YOU REPRESENT THAT YOU HAVE FULFILLED ANY RIGHT OF REVIEW OR OTHER OBLIGATIONS REQUIRED BY SUCH CONTRACT OR AGREEMENT. LAU will clearly identify your name(s) as the author(s) or owner(s) of the submission, and will not make any alteration, other than as allowed by this license, to your submission.

Name: Sandra Abdellatef

Signature: [redacted] Date: 08 / 04 / 2019
(Day / Month / Year)

LAU
الجامعة اللبنانية الأميركية
Lebanese American University

PLAGIARISM POLICY COMPLIANCE STATEMENT

I certify that:

1. I have read and understood LAU's Plagiarism Policy.
2. I understand that failure to comply with this Policy can lead to academic and disciplinary actions against me.
3. This work is substantially my own, and to the extent that any part of this work is not my own I have indicated that by acknowledging its sources.

Name: Sandra Abdellatef

Signature: [redacted]

Date: 08 / 04 / 2019
Day Month Year

Dedication Page

To my safety net, my supportive father

To my sun, my loving mother

To my heart and soul, Ammar & Mayar

Acknowledgements

First, I want to thank my supportive family, you give me strength, and I couldn't be where I am today without you.

I would like to emphasis on the effort put on this research by the most inspirational mentor Dr. Mirvat El-Sibai. This research would have not seen the light without your relentless guidance. You taught me how to be passionate and sincere. I cannot be grateful enough for the blessing of being a student of yours.

I would also like to sincerely thank the Dean of Arts and Sciences Dr. Constantine Daher, the Chairperson of the Biology department Dr. Sima Tokajian, all of the faculty members of the Biology department Dr. Ralph Abi-Habib, Dr. Roy Khalaf, Dr. Sama Sleiman, Dr. Michella Ghassibe, and to the thesis committee members Dr. Roy Khalaf, and Dr. Tarek Nawas.

I am also grateful to Mrs. Hanan Naccash, Mrs. Sawsan Jabi, Ms. Maya Farah, and Ms. Helena Bou Farah for their technical support and help.

I thank my colleagues in the Biology graduate program especially past and present members of the El-Sibai lab.

Distinctive Role of StarD13 in Serous Ovarian Carcinoma Cell Proliferation, Metastasis, and Invadopodia Assembly

Sandra Abdullatef

Abstract

Ovarian carcinoma is the second most leading cause of deaths among female reproductive system malignant tumors. Serous epithelial carcinomas have a poor treatment rates for it is most likely to be advanced when diagnosed due to its poor indications and symptoms. Ovarian serous carcinomas are mainly divided into different stages according to the invasiveness and metastatic ability of the tumor. Many mutations are acquired which lead to the development of this malignancy. This occur in entities that greatly affect the cell cycle, cell signaling pathways and cell motility, which all involve the action of Rho GTPases. The protein of interest in the present study was DLC2, also known as StarD13 or START-GAP2, a GTPase-activating protein (GAP) for Rhoa and Cdc42. Literature data indicate that this protein is considered a tumor-suppressor in hepatocellular carcinoma. Previous research in our laboratory confirmed StarD13 as a tumor suppressor in astrocytoma, in breast cancer, and in colon cancer. In this study, we aim to investigate the role of StarD13 in cell migration, invasion, and proliferation. The results show that StarD13 is a tumor suppressor in ovarian serous carcinoma, it inhibits the function of cdc42 leading to the decrease in invadopodia assembly hence hindering invasion. StarD13 is needed for cell motility via its indirect effect on RhoA activation cycle. Moreover, StarD13 knockdown increased cell adhesiveness via the crosstalk between Cdc42 and Rac1 pathway. Therefore the cells were not being able to detach and move. Establishing the conclusion that StarD13 is in fact a tumor suppressor but it is needed for cell motility in ovarian cancer.

Keywords: StarD14, RhoA, Cdc42, Invadopodia, Focal Adhesions, Ovarian Serous Carcinoma, Motility.

TABLE OF CONTENTS

LIST OF FIGURES.....xii

LIST OF ABBREVIATIONS.....xiii

Chapter One Literature Review.....1

1.1 Cancer…….....1

1.1.1 Overview…….…1

1.1.2 Tumorginesis……....2

1.2 Ovarian Cancer 4

1.2.1 Statistics and Epidemiology 4

1.2.2 The definition of ovarian cancer and classification 5

1.3 Cell Motility and Invasion.....7

1.3.1 Cell Motility 7

1.3.2 Epithelial to Mesenchymal Transition (EMT).....9

1.3.3 Ovarian Cancer Cell Metastasis……..9

1.3.3 Invasion And Invadopodia Assembly……10

1.4 The Rho family of GTPases 12

1.4.1 General overview.....12

1.4.2 The Rho Family of GTPases Regulators……....13

1.4.3 The Rho Family of GTPases effectors…..……..15

1.5 RhoA and Cdc42.....16

1.6 StarD13……..19

1.7 Purpose of the Study 20

Chapter Two Materials and methods 22

2.1 Cell culture 22

2.2 Antibodies and reagents 22

2.3 Cell transfection with siRNA 22

2.4 Western immunoblotting 23

2.5 Cell proliferation reagent (WST-1)..... 23

2.6 Adhesion assay ……24

2.7 Invasion Assay 24

2.8 wound healing assay.....25

2.9 motility assay 25

2.10 Immunocytochemistry…..……..26

2.11 Live upshift assay……..26

2.12 Pull-down assay……27

2.13 Quantitation of focal adhesions ……27

Chapter Three Results…….…….…….….22

3.1 Knocking down StarD13 using Si-RNA…….……22

3.2 StarD13 is a tumor suppressor…….…....22

3.3 The role of StarD13 on ovarian cancer cell 2D motility.....30

3.3.1. StarD13 depletion decreases human ovarian cancer SKOV3 cell migration. However the knockdown of StarD13 increased cell migration in human ovarian cancer cell line CAOV3……30

3.3.2 StarD13 knockdown decreases adhesion to collagen in human ovarian cancer SKOV3 cell line. However, the knockdown of StarD13 increased adhesion in CAOV3 and PA-1 ovarian cancer cell lines……..31

3.4 StarD13 is has a GAP activity for Cdc42 but not for RhoA……...34

3.5 the effect of StarD13 depletion on the formation of focal adhesion……34

3.6 StarD13 has a negative effect on the formation of ovarian cancer cells ruffles and protrusions…….36

3.6.1 EGF stimulation had no measurable effect on the size of SKOV3 cells but clear increase in the cell ruffling was observed. …….……..36

3.7 StarD13 is responsible for cell invasion regression in serous ovarian carcinoma SKOV3 cells and the depletion of StarD13 lead to the decrease in the number of invadopodia assembled. ……..……...38

3.7.1 StarD13 depletion promoted the invasion of SKOV3 cells……..38

3.7.2 StarD13 depletion promoted the assembly of Cdc42 induced invadopodia…….….39

Chapter Four Discussion 50

Chapter Five Conclusions 56

Bibliography 58

LIST OF FIGURES

Figure Page

Figure 1: Stages of Tumorigenesis..... 2

Figure 2: Hallmarks of Cancer. 4

Figure 3: cell motility cycle. 8

Figure 4: Invadopodia formation.....12

Figure 5: The regulation diagram of typical Rho GTPases……14

Figure 6: The downstream effectors of the classic Rho GTPases.....16

Figure 7: Cdc42 and its effectors in invadopodia assembly. 18

Figure 8: cell motility: RhoA activation cycle regulated by StarD13..….....20

Figure 9: western immunoblotting to determine the expression of StarD13 in several ovarian cancer cell lines. 29

Figure 10: StarD13 decrease cell viability playing its role as a tumor suppressor.....29

Figure 11: StarD13 is a Cdc42 GAP but not a GAP for RhoA in SKOV3/CAOV3 cell lines:.....32

Figure 12: the effect of StarD13 Knockdown on cell motility.....33

Figure 13: wound healing assays of ovarian cancer cells SKOV3, and CAOV3 after transfection with si-RNA of StarD13 and control at time zero and after 24hours of forming the wound.....33

Figure 14: FigureStarD13 knockdown effect on the formation of focal adhesion....34

Figure 15: the effect of StarD13 knockdown on cell adhesion to collagen…...35

Figure 16: StarD13 negatively regulate EGF stimulated protrusions in SKOV3 cells by deactivating Cdc42…….....37

Figure 17: StarD13 depletion in SKOV3 cells promotes cellular invasion.....39

Figure 18: Immunocytochemistry of Cotrtactin to depict the number of invadopodia upon the depletion of StarD13 in ovarian cancer cell line SKO..... 41

Figure 19: Immunocytochemistry of Tks4 to depict the number of invadopodia upon the depletion of StarD13……..... 42

Figure 20: Immunocytochemistry of Wasp to depict the number of invadopodia upon the depletion of StarD13 in ovarian cancer cell line SKOV3……..…43

Figure21: the role of StarD13 in SKOV3 Ovarian Cancer…….……49

LIST OF ABBREVIATIONS

Arp2/3: Actin-related protein 2/3

BSA: Bovine Serum Albumin

Cdc42: Cell division cycle 42

CRIB: Cdc42/Rac interactive binding

DMEM: Dulbecco's Modified Eagle Medium

ECL: Enhanced Chemiluminescence

ECM: Extracellular matrix

EGF: Epidermal Growth Factor

EMT: Epithelial-mesenchymal transition

FAK: Focal Adhesion Kinase

FBS: Fetal Bovine Serum

GAP: GTPase Activating Protein

GDI: Guanine Nucleotide Dissociation Inhibitor

GDP: Guanosine diphosphate

GEF: Guanine Nucleotide Exchange Factor

GTP: Guanosine triphosphate

GTPase: Guanosine triphosphatase

HEPES: 4-(2-hydroxyethyl)-1-piperazineethanesulfonic acid

HGF: Hepatocyte Growth Factor

LIMK: LIM kinase

MAP2: microtubule-associated protein 2

mDia: Mammalian homolog of diaphanous

MLC: Myosin Light Chain

MLCK: Myosin Light Chain Kinase

MMP: Matrix metalloproteinase

MT-MMP: Membrane-type matrix metalloproteinase

NHE1: Na+/H+ Exchanger

PAK: p21 activated kinases

PBS: Phosphate Buffered Saline

PDGF: Platelet-derived Growth Factor

PI3K: Phosphatidylinositol 3-kinase

PIP2: Phosphatidyl 4,5-bisphosphate

PIP3: phosphatidylinositol (3,4,5)-triphosphate

PVDF: Polyvinylidene fluoride

Rac1: Ras-related C3 botulinum toxin substrate 1

Ras: Rat sarcoma

RBD: Rhotekin binding domain

RhoA: Ras homologous member A

RhoBTB: Rho-related BTB domain-containing protein 1

RhoC: Ras homologous member C

RhoD: Ras homologous member D

RhoF: Ras homologous member F

RhoG: Ras homologous member G

RhoH: Ras homologous member H

RhoJ: Ras homologous member J

RhoQ: Ras homologous member Q

RhoU: Ras homologous member U

RhoV: Ras homologous member V

ROCK: Rho Kinase

ROI: Region of interest

SDS-PAGE: Sodium Dodecyl Sulfate Polyacrylamide Gel Electrophoresis

siRNA: Small interfering Ribonucleic Acid

TGF-β: Transforming Growth Factor beta

Tks4: SH3 and PX domains 2B

Tks5: SH3 and PX domains 2A

WASP: Wiskott - Aldrich syndrome Protein

WAVE: WASP-Family Verprolin-Homologous

WAVE1: WASP-family verprolin homologous protein 1

WHO: World Health Organization

Chapter One

Literature Review

1.1. Cancer

1.1.1. Overview

Cancer is considered one of the most threatening global diseases; it is the second most prominent cause of death in the United States. Accounting for approximately 606,880 deaths and 1,762,450 new cancer cases in 2019 (Siegel, Miller, & Jemal, 2019).

Genetic aberrations that cause the cells to grow uncontrollably, proliferate indefinitely, and acquire invasiveness and motility to locations occupied by normal cells, Is the definition of cancer according to American Cancer Society. While the origins of cancer are not completely understood, nonetheless some of the most important factors that attribute to increase the incidence of cancer, whereas working simultaneously or gradually, are classified into the amendable factors such as obesity, tobacco. And the unchangeable factors the genetically acquired mutations ("Cancer Facts & Figures 2019 | American Cancer Society," 2019).

Tumors are classified into benign innocuous, or cancerous malignant. Benign tumors are restricted to the site of origins without invading bordering tissues. Unlike cancerous tumors that are equipped with metastatic abilities enabling it to invade and transgress through circulation and lymphatic system (National Cancer Institute, 2015).

1.1.2. Tumorigenesis

The accumulation of mutations and the unlimited possibilities in rearranging the genome, in addition to the different body organs each with its distinctive functions, imputes the complexity of cancer (Hanahan, 2014).

Organ tissues are normally exposed to different mutations. These mutations are subjected to clonal expansion while the tissue's cells proliferate. Only distinctive number of mutations could lead to tumorigenesis. The expansion of mutations in a normal cell lineage driving the replacement of cancerous cell population in lieu of somatic cell population is called field cancerization that drives the development of malignant tumor. Cancerized lineage is a population of cells bearing survival advantages over somatic cell population, however cancerized linage does not have enough characteristics to produce malignant tumors (Curtius, Wright, & Graham, 2018).

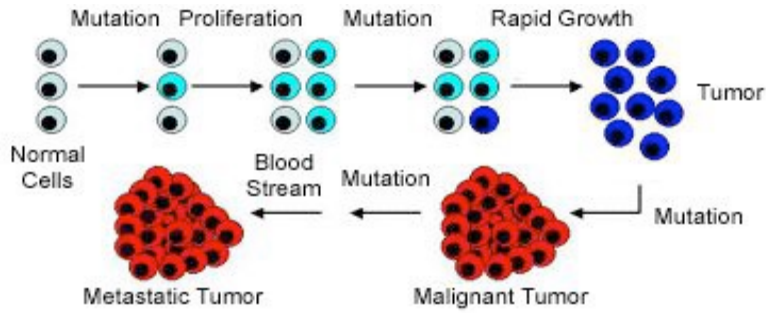

Fig. 1. Stages of Tumor Progression. Normal cells are exposed to single cell mutation (light blue). Clonal expansion of mutation occurs with proliferation of the cells. Further exposure to mutagens develops selective proliferative advantages over somatic cells (dark blue). Leading to the replacement of normal cells. This cancerized lineage develops additional mutations driving the once innocuous tumor to a malignant invading tumor. (Red) (Source: Jay D. Hunt, LSU Health Sciences Center, n.d.).

In order for the tumor to be malignant and cause metastatic cancer, ten essential properties must be obtained by the tumor illustrated in Hanahan and Weinberg's model of cancer's hallmarks (Figure 2). These hallmarks provide a logical systematizing instrument to distinguish between numerous neoplastic diseases (Hanahan & Weinberg, 2000).

These capabilities are obtained in line with the progression of the tumor, and include: the ability to resist cell death, proliferate indefinitely, acquire mutations via genome flexibility achieved through genome instability, evading growth suppressors, sustaining proliferative signaling, inducing angiogenesis, invasion and metastatic abilities, inflammation, deregulation of cell energetics and metabolism, and avoiding immune defenses. In addition, another added level of complexity is depicted in tumors by the presence of somatic cells that participate in the acquisition of these hallmarks through creating the microenvironment suitable for tumor progression (Hanahan & Weinberg, 2011).

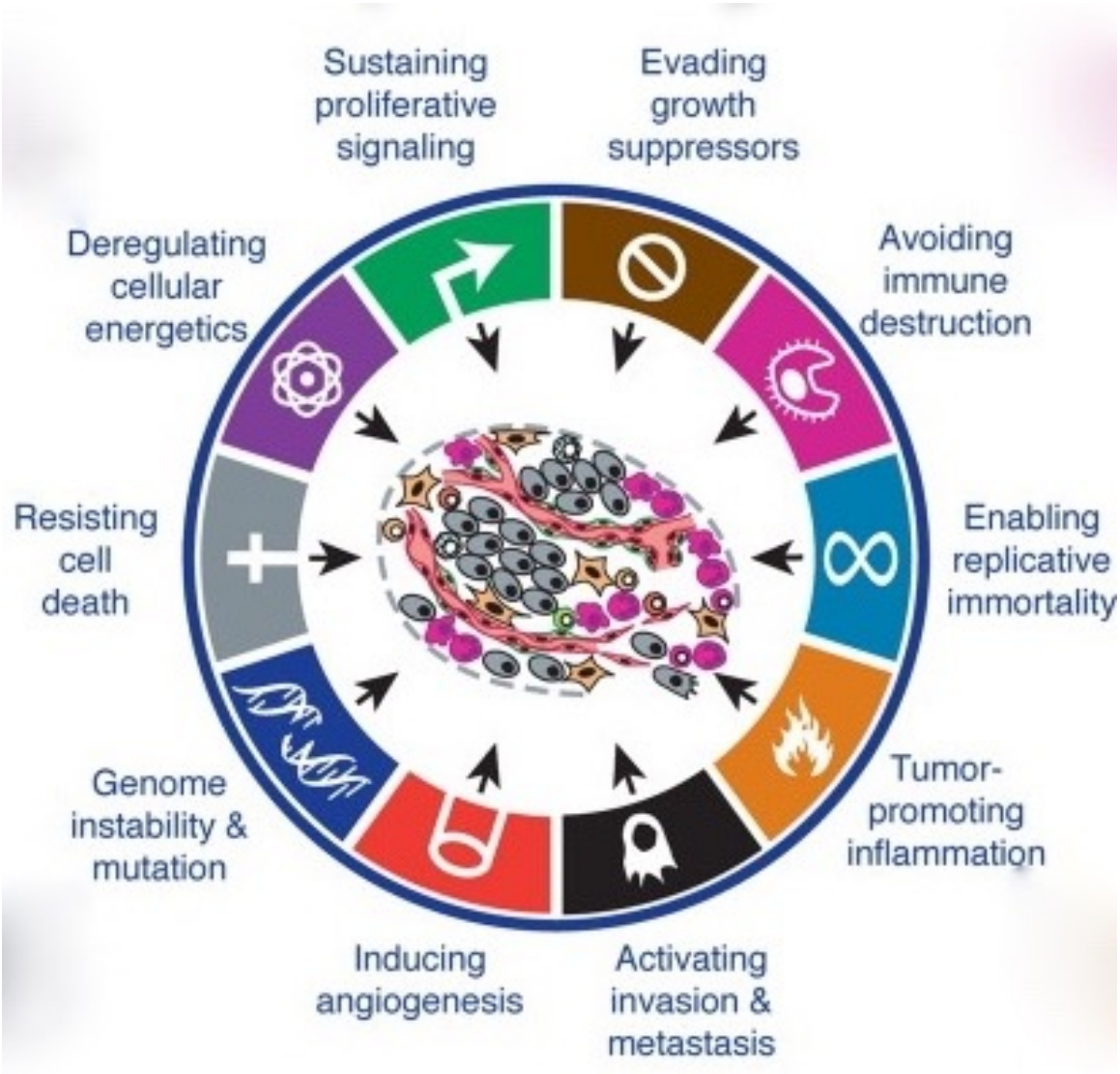

Fig. 2. The Hallmarks of Cancer: (Source: Hanahan & Weinberg, 2011).

1.2. Ovarian Cancer

1.2.1. Statistic and Epidemiology

Ovarian cancer is responsible for most of the mortalities among female reproductive system cancer, and considered in females the fifth most leading cause of cancer deaths (Torre et al., 2018).

According to The American Cancer Society there will be in 2019 approximately 22,530 new diagnosed cases of ovarian cancer, and 13.980 ovarian cancer deaths, with a risk factor of having ovarian cancer of one for every seventy-eight females, and a mortality rate of one for every hundred and eight women. Additionally, more than half of the diagnosed cases are of women above sixty-three years old ("Key Statistics for Ovarian Cancer," n.d.).

Furthermore, it is more common in Caucasian females compared to African-American females. Besides, low incidences have been reported for Asian women. The survival rate is the lowest amid African-Americans women. Most of the incidences are irregular and random with only five to ten percent recognized as familial (Holschneider & Berek, 2000).

Ovarian cancer consists of dissimilar malignant tumors that differ in their original cause of formation, and the molecular basis of development. Epithelial ovarian cancer accounts for 85% to 90% (Torre et al., 2018).

1.2.2. The definition of ovarian cancer and classification

The female reproductive glands that are responsible for the production and secretion of eggs are the ovaries. The ovaries consist of three types of cells each with the possibility of arising into different type of tumor. The most common tumor of the ovarian tissue is the epithelial tumor that develops from the epithelial outer lining of the ovaries. Tumors could also arise from the cells that are responsible for the production of the ova; these tumors are called germ cell tumors. The last type of ovarian cancer tumors are the stromal tumor, which grow out of the tissue that support the ovaries together ("What Is Ovarian Cancer?," 2019).

Most of the epithelial ovarian tumors are innocuous and branched into several types such as Brenner tumors, serous, and mucinous adenomas. In addition to the low malignant potential (LMP) tumors that are indistinguishable as cancerous or not under the microscope ("Types & Stages - National Ovarian Cancer Coalition," n.d.).

Malignant ovarian tumors are called carcinomas and encompass mostly of epithelial carcinomas. Epithelial carcinomas can further be classified into different kinds based on the cell histology under the microscope. The most common type with a 52 % is the serous epithelial carcinoma, then the endometrioid carcinomas with 10%, and 6% for each clear cell and mucinous carcinomas. The rest is classified as unspecified rare type ("Ovarian Epithelial, Fallopian Tube, and Primary Peritoneal Cancer Symptoms, Tests, Prognosis, Stages," 2016).

Furthermore, ovarian carcinomas are graded based on its morphology compared to normal tissues. Grade I carcinomas resemble the normal cells, whereas

grade III have a worse prognosis and less likely to resemble normal cells ("What Is Ovarian Cancer?," 2019).

In addition, carcinomas are further classified based on other features such as their metastatic abilities and their response to treatment. Type I (e.g. grade I serous, grade I clear cell, and also grade I mucinous carcinomas), is more genetically stable, tends to grow slower, and has a poor response to chemotherapy compared to type II (e.g. Grade III serous carcinoma) (Robert J. Kurman & Shih, 2016). Moreover, type I is assumed to develop from innocuous lesions originated outside the ovaries that are later implanted in ovary, and exposed to several mutations to become cancerous (Torre et al., 2018). While the type II is originated at the fimbriae of the fallopian tubes that later metastasized restrictively to the ovaries, peritoneum, or to both sites (R. J. Kurman, 2013).

1.3 Cell Motility And Invasion

1.3.1 Cell motility

Normal cells depict a motility behavior throughout several physiological events, such as embryogenesis, cell development and wound healing, also during an inflammatory response (Pollard & Borisy, 2003). Cancerous cells employ the same strategies used for cell motility in order to acquire invasiveness (Hanna & El-Sibai, 2013).

Nowadays, the interest of oncology is directed towards underlying the mechanisms and signaling pathways through which cancer cells promote tumor growth, invasion, and metastasis (Lauffenburger & Horwitz, 1996).

The spread of cancerous cells from the site of formation to adjacent tissues and to other organs, which is responsible for 90% of cancer mortalities and morbidities, is defined as cell Metastasis (Tarin, 2011).

Chemo-taxis is the initial trigger of cell motility; it begins with a stimulus such as chemo attractant, repellent, or growth factor, released at the cell's extracellular matrix, recognized by the cell surface membrane receptors, triggering a cascade of signals guiding the cell towards the direction of chemo attractant, or opposing the direction of stimulus if the trigger is a chemo-repellant. The movement of the cell starts with the formation of protrusions via actin filaments rearrangement and the polymerization of novel filaments. Then, these protrusions are stabilized to the extracellular matrix (ECM) through the creation of focal points and adhesive

structures, which enable the formation of a mechanical force, that is needed for the cell's locomotion, at the same time the cell's rear edge and tailing must de-adhere enabling the cell to use the mechanical pull to retract and move (Ananthakrishnan & Ehrlicher, 2007).

In conclusion, the steps of cell motility include: protrusion formation, adhesion, trailing retraction, de-adhesion (Bailly & Condeelis, 2002). (Figure 3).

Additionally, Actin is abundant in eukaryotic cells and it is the main component needed for the formation of protrusion-rich lamellipodium at the cells 'edges (Pollard & Borisy, 2003). Cell directional motility is also a property depicted by lamellipodium; hence cells don't exclusively manifest this process (Verkhovsky, Svitkina, & Borisy, 1999).

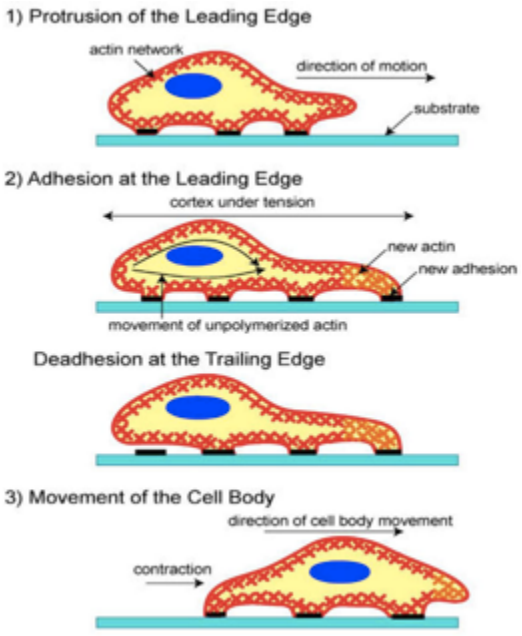

Figure 3: cell motility cycle: triggered by an extracellular stimulus the cell forms protrusions in the direction of motion, stabilized by adhering to the substrate at the leading edge, while simultaneously de-adhering at the cell's tail, allowing the cell to

move due to the contractile force form (source: Ananthakrishnan & Ehrlicher, 2007).

1.3.2 Epithelial to Mesenchymal Transition (EMT)

The accumulation of mutations in epithelial cells or epithelial stem cells that add mesenchyme like properties, aid in the transformation of epithelial cells into metastatic cells (Chaffer & Weinberg, 2011). Further alterations occur during tumor progression to cause the cancerous cells to metastasis locally through EMT mode, while the basement membrane is disrupted. Eventually allowing the metastatic cells to intravasate via circulation or lymph vascularization, facilitating the migration to distant organs. When the metastatic cells arrive to secondary sites, these cells can from new malignant tumors or persist to their state as micro-metastatic cells (Thiery, 2002).

1.3.3Ovarian Cancer Cell Metastasis

Ovarian carcinomas disseminate mostly through the formation of ascites instead of the conventional route via circulation. This is due to the fact that ovarian cancer is solely superficially invasive and metastasis within the peritoneum (Lengyel, 2010).

Even though the most common route of metastasis of ovarian cancer is via passive dissemination, traces of metastatic tumors were evident in the omentum, and other distant sites. Therefore indicating the intravasation of the blood vessels by

ovarian carcinoma to migrate and invade distant organs through EMT (Akin et al., 2008).

Accordingly, There are two mechanisms of ovarian cancer metastasis. Due to the fact that most ovarian carcinomas develop from the epithelial tissues, these carcinomas depict an EMT mode of migration to invade distant tissues, or passively disseminate via Spheroids that flow along the peritoneal fluid and exert a specific attachment patterns to the peritoneum. Afterwards, these ovarian cancerous suspended cells restore their epithelial characteristics. Higher-grade metastatic ovarian cells are characterized by the formation of tumor nodules at secondary sites causing bowl obstruction, ascites, and severe wasting of the organism (Lengyel, 2010).

Moreover, Tumor suppressor gene mutations (e.g. P53, nm23), promotes Passive dissemination via the peritoneum (Mandai et al., 1995). Furthermore, integrins, cadherins, CD44 adhesion molecules, metaloproteases, and cytokines affect passive dissemination of ovarian cancer (Bernstein & Liotta, 1994; Horiuchi et al., 2003; Zhan et al., 2012)

1.3.4 Invasion And Invadopodia Assembly

The actin rich structures required for the cancer cell to migrate and invade are lamellipodia, filopodia, and invadopodia. Lamellipodia and filopodia are essential structures for the two-dimensional motility pattern, and are vital in guiding the cell in direction-oriented motion. These structures form at the leading edge of the metastatic cell. Nonetheless, invadopodia play an essential role in degrading the extracellular matrix and formation of invading projections to achieve the three-dimensional migration pattern (Alblazi & Siar, 2015).

Invasive cancer cells assemble invadopodia, which are characterized by their location at the basal membrane, and their ability to form dysmorphic sized projections that are rich in filamentous actin (Eddy, Weidmann, Sharma, & Condeelis, 2017). These projections gather within a number of modulators, for instance: Cortactin, Tks4, N-WASP, Arp2/3 (Beaty & Condeelis, 2014; Yamaguchi, 2012).

The precursor of invadopodia formation and assembly is confined in the following stimulating signals, the activation of matrix metalloproteinase (MMP), further oncogenic transformation of the ovarian carcinoma, the presence of growth factors (EGF, PDGF, TGF-β), the stimulation of Epithelial to Mesenchymal transition (Clark, Whigham, Yarbrough, & Weaver, 2007)(Hideki Yamaguchi et al., 2005).

The assembly of invadopodia is covered in multistep mechanism (Figure 4). Initially N-WASP, cofilin, and Arp 2/3 complex must be recruited to the site of actin-cortactin complex in order to construct the core of invadopodia (Beaty & Condeelis, 2014a). Afterwards, Tks4 plays an important role as an anchorage of the formed core to PIP2 in the plasma membrane. Attaching this complex to the plasma membrane trigger the tethering of adhesion receptor β1 integrin to the stabilized core, further leading the core binding to the extracellular matrix entities, aiming to stabilize the so far assembled structure (Eddy et al., 2017). Once the core is stabilized through its attachment to the ECM and the plasma membrane, NHE-1-cofilin pathway is activated, leading to the polymerization of actin filaments, which provides the assembled projection with further elongation. Lastly, full elongation is achieved due to microtubules employed to the site of assembly. Concurrently,

metalo-proteases recruitment leads to the degradation of the extracellular matrix facilitating the invasion process (Sharma et al., 2013). (Figure4).

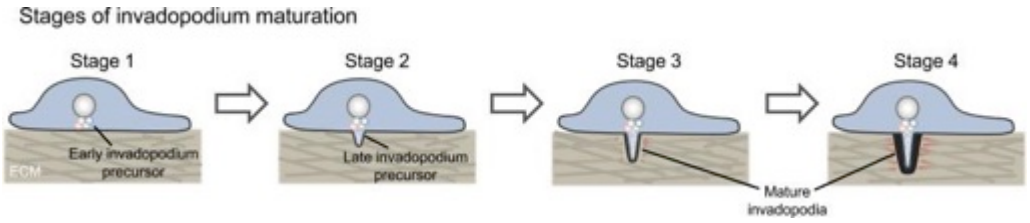

Fig. 4. Invadopodia formation. (Source: Beaty & Condeelis, 2014)

1.4 The Rho family of GTPases

1.4.1 General overview

One of the most important proteins regulating cell motility is the Rho family of GTPases. This family consists of small GTP binding proteins their size ranges between 20 and 40 KDa. Many GTPases, which belong to this family, are involved in actin cytoskeleton regulation and remodeling (Ju & Gilkes, 2018).

Around 1980, RAS gene was first discovered from the Rous sarcoma virus (Takai, Sasaki, & Matozaki, 2001). Within the Ras superfamily resides 130 proteins that belong to Ras, Rho, Arf/Sar1 and Rab/Ran-subfamilies (Ananthakrishnan & Ehrlicher, 2007).

The Rho family of GTPases has 23 proteins categorized based on genome sequence similarities into eight subgroups: Rho homologues, RhoB, Cdc42/RhoQ/RhoJ, RhoF/RhoD, Rac/RhoG, Rnd, RhoH, RhoU/RhoV and RhoBTB. All of those proteins play a distinctive role but have similarities in amino acid sequence (Lawson & Ridley, 2018).

Furthermore, this family of proteins is further classified based on their affinity of binding to ATP into typical (such as RhoA, Cdc42, and Rac1), and atypical (Rnd subfamily, and RHOH). Out of all Rho GTPases' proteins, the classic

Cdc42, Rac1, and RhoA were studied thoroughly (Haga & Ridley, 2016).

The cross talk between the Rho GTPases affects cellular signal transduction pathways, cytoskeleton organization, motility, polarity, and invasion (Sahai & Marshall, 2002).

1.4.2 The Rho Family of GTPases Regulators

The Rho GTPases play the role of a molecular switch that shifts between an active form when bound to GTP, and the inactive form when the GTP bound is hydrolyzed into GDP (Mackay & Hall, 1998).

Most of the Rho GTPases, are characterized by their facilitated movement between the cell cytoskeleton and the cell membrane, which is due to their C-terminus modifications achieved by Isoprenoid (Mitin, Roberts, Chenette, & Der, 2012).

Rho GEFs are the guanine nucleotide exchange factors, which are a positive regulator of the typical Rho GTPases by triggering the trade of the bound GDP in the inactive form for GTP to activate Rac1, Cdc42, and RhoA. Rho GEF consists of two domains the activating domain (Dbl homology domain: DH), and the inhibitory domain (pleckstrin homology domain: PH) .The inhibitory domain binds to the activating domain, blocking its catalytic activity. The trigger of the signal transduction Pathway PI3K promotes the phosphorylation of the phospholipid component of the plasma membrane PIP2, which supports the blockage of DH by PH domain. Upon stimulation of the PI3K, PIP2 is phosphorylated to yield PIP3 that

favors the binding to the GEF's DH domain activating the GEF (Bustelo, 2000; Zhou & Snider, 2006). Also, the trans membrane receptor integrin helps activate Rho GTPases by the recruitment of FAK (focal adhesion kinase). When phosphorylated FAK forms the Src binding site. Then this complex aids in paxillin and Cas phosphorylation, which in turn promotes the activation of Rac and the inhibition of RhoA (Lawson & Burridge, 2014; Ruest, Roy, Shi, Mernaugh, & Hanks, 2000; Tomar, Lim, Lim, & Schlaepfer, 2009).

Rho GAPs are the GTPases activating proteins, the negative regulators as they catalyze the hydrolysis of the bound GTP to GDP and inactivate the Rho GTPase (Bos, Rehmann, & Wittinghofer, 2007).

Finally, the GDIs are guanine nucleotide dissociation inhibitors, there are three known GDIs, which regulate the typical Rho GTPases by stabilizing the GDP bound inactive form (Van Aelst & D'Souza-Schorey, 1997). (Figure5). Furthermore, GDI's have a frail affinity to GTP that accounts for the inhibition of GTPases through blocking at the exchange step and at the hydrolysis step (Hart et al., 1992). In addition to their role as regulators, the GAPs and GEFs depict a part in Rho GTPase -mediated cell migration (Goicoechea, Awadia, & Garcia-Mata, 2014).

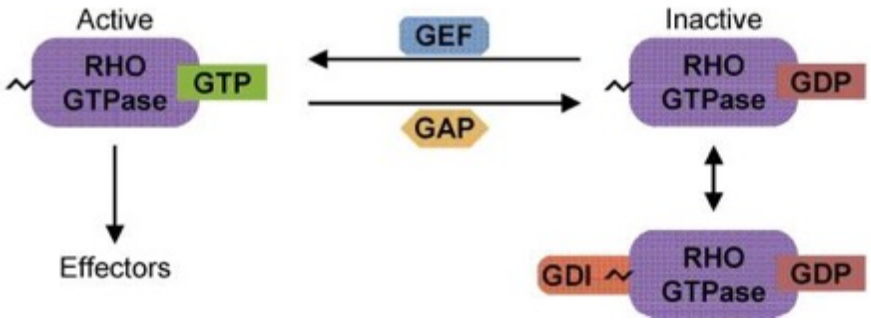

Fig. 5. The regulation diagram of typical Rho GTPases. GEFs stimulate the exchange of GDP to GTP activating the GTPases. GAPs catalysis the hydrolysis of GTP into GDP deactivating the

GTPases. While the GDIs stabilize the inactive form by binding to the GTPases' isoprenyl, which is responsible for the binding of GTPases to plasma membrane. Source: (Lawson & Ridley, 2018).

Post translation modifications, rather than the cycling of GTP and GDP, mainly achieve the regulation of the atypical Rho GTPases, such as lipid modifications. In addition, to the regulation via ubiquitilation, expression, and proteasome degradation (Blom, 2017; Haga & Ridley, 2016).

1.4.3 The Rho Family of GTPases effectors

Downstream of RhoA, the serine-threonine kinases ROCKs play an important role in increasing the contractility through the phosphorylation of the myosin light chain (MLC), and stabilize the actin filaments through the phosphorylation of LIM kinases and cofilin inactivation. Additionally, ROCKs or Rho kinase are found to play an essential part in cell invasion and migration (Olson & Sahai, 2008). Furthermore, ROCK is found to be an important regulator of cell propagation, cell death, the transformation of an oncogene, and in transcription (Rath & Olson, 2012).

Downstream of Rac1 and Cdc42, the threonine-serine kinase effectors responsible for driving several signaling pathways that acquire the cell with oncogenic features, is the P21 associated kinase Pak (King, Nicholas, & Wells, 2014; Radu, Semenova, Kosoff, & Chernoff, 2014). During metastasis, the phosphorylation of LIMK by Pak1 leads to the stabilization and remodeling of actin filaments in order for the lamellipodia to form at the leading edge of the cell (Yang et al., 1998). Furthermore, Pak1 phosphorylate Paxillin in order to prompt focal

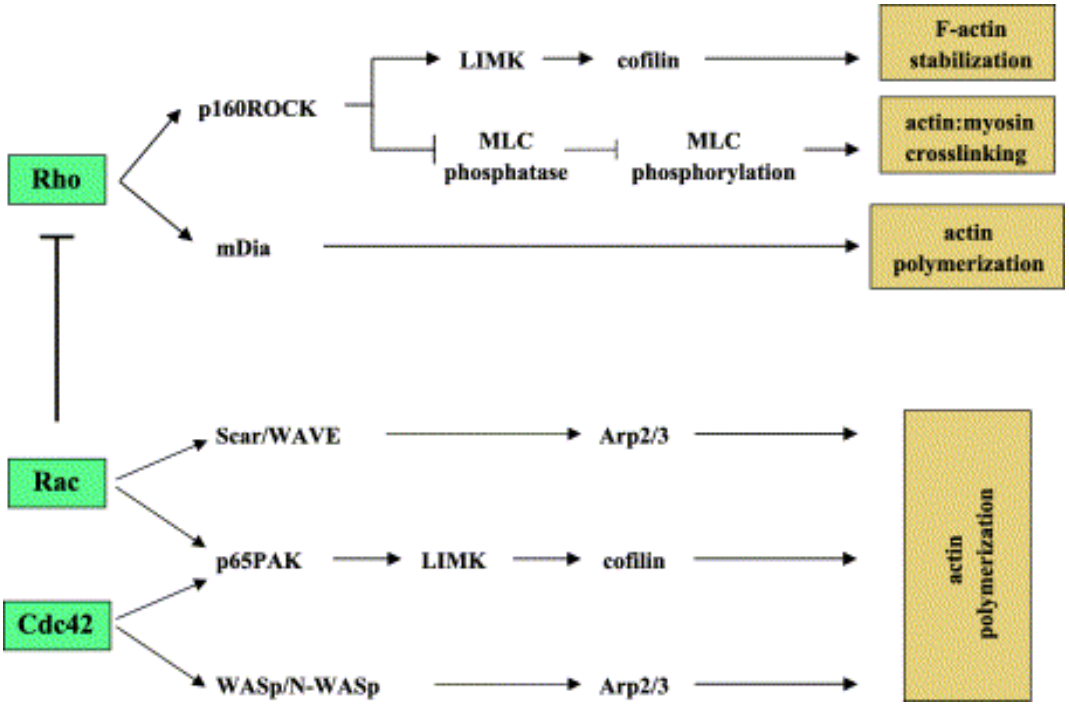

contacts at the cell's leading edge

(Delorme-Walker et al., 2011). Pak's also stimulate cell proliferation by the activation of several signaling pathways involved in cell progression, such as Erk, PI3K/AKT,and Wnt (Radu et al., 2014). Additionally to the previous kinase effectors, well studies scaffolding proteins such as WASP, N-WASP and WAVE play the role of effectors downstream of Rac1 and Cdc42. These proteins trigger Arp2/3 that is responsible for the formation of novel actin filaments at the leading edge of the cell, which in turn promotes the formation of filopodia and lamellipodia aiding the cell migration (Lane, Martin, Weeks, & Jiang, 2014). (Figure6).

Fig. 6. The downstream effectors of the classic Rho GTPases.
Source: (Raftopoulou & Hall, 2004).

Messenger RNA levels of RhoA and RhoC in serous ovarian carcinomas are higher compared to benign ovarian tumors and normal tissues combined. While the protein levels of RhoA is increased in ovarian carcinomas, the GDIs and ROCK expression levels are stable (Horiuchi et al., 2003).

1.5 RhoA and Cdc42

The common effector amongst all the stages of tumor progression is RhoA. RhoA drives cell cycle progression angiogenesis, local cell invasion, finally cell migration. Thoroughly, the activation of RhoA requires the stimulation of trans membrane G-Coupled Protein Receptors and Tyrosine Kinase Receptors. After the receptor stimulation, it activates Rho GEFs, which in turn activates RhoA.

Afterwards RhoA interacts with several downstream effectors such as ROCK and PAKs to drive the formation of stress fibers, adhesive structures, and actomyosin contractility. Or mDia in order to drive the actin polymerization (Haga & Ridley, 2016).

In addition, the role of RhoA in actin nucleation was thought to be restricted only to the cell's rear end. But further investigation indicated that RhoA is actually active at the leading edge of the motile cell signifying the additional role of RhoA in the formation of lamellipodia and cell ruffles (El-Sibai et al., 2008). Focal points must mature into focal adhesions through the inactivation of Rac1 and the activation of RhoA. In order for the cell to move, RhoA must enter a cycle of activation and deactivation opposing the activation of Rac1 (Khalil et al., 2014).

Cdc42 a classic Rho GTPase if its level of expressions is controlled and the normal level of its effectors is maintained, it can cease the progression of cancer (Qadir, Parveen, & Ali, 2015). Cdc42's first discovery was in the yeast *Saccharomyces cerevisiae.* It plays many essential roles in eukaryotic cells including cell division, transformation, invasiveness, metastasis, catalyzing enzymes and cellular polarity (Johnson & Pringle, 1990; Qadir et al., 2015).

The role of Cdc42 in cancer is actually more complex and comprises the stimulation of numerous signaling pathways (Martin et al., 2016), and the modulation of transcription factors such as SRF (Hill, Wynne, & Treisman, 1995), and NFkB (Perona et al., 1997). Overexpressed levels of Cdc42 were observed in a multiple carcinomas such as non-small cell lung (Liu et al., 2009), melanoma (Tucci et al., 2007), breast and testicular (K. Stengel & Zheng, 2011; Fidyk, Wang, & Cerione, 2006). These observations lead to the assumption that Cdc42 works as an

oncogene in malignant tumors and must be therapeutically targeted. Cdc42 promotes invadopodia assembly by driving actin nucleation through the activation of N-WASP and ARP complexes (Stengel & Zheng, 2011). In addition, Cdc42 promotes the activation and production of metalloproteinase that degrades the extracellular matrix components facilitating the process of invasion (Hideki Yamaguchi et al., 2005).

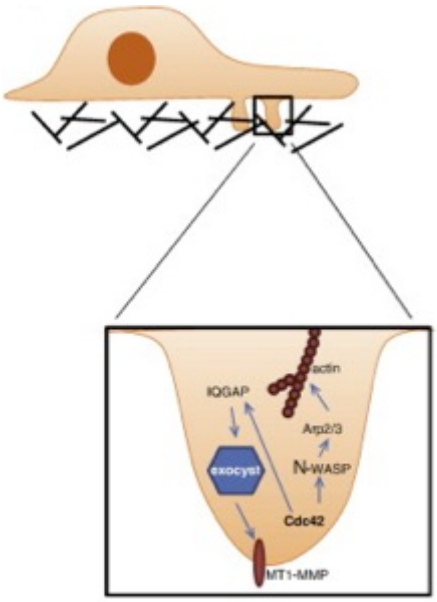

Cdc42 was shown to drive the assembly of invadopodia in breast cancer through boosting the CIP4 signaling, eventually increasing the activation of N-WASP resulting in high levels of invadopodia formation (Pichot et al., 2010). (Figure7).

Figure 7: Cdc42 and its effectors in invadopodia assembly. Cdc42 binds the Ras GTPase-activating-like protein (IQGAP) to the exocyst that is involved in cell trafficking. This binding promotes the production of mettle-proteinases and targeting the MMPs to the tip of the invading protrusions acting on degrading the membrane. Cdc42 forms the protrusions through activating the N-WASP and ARP complexes (source: Stengel & Zheng, 2011).

1.6 StarD13

StarD13 or deleted liver cancer (DLC2) also called START-GAP2 was firstly identified by Ching *et al*, and found to be a Rho GAP for Cdc42 and RhoA but not for Rac in Hepatocellular carcinoma (Ching et al., 2003), and in astrocytoma (El-Sitt et al., 2012). Furthermore, it is one of three Rho GAPs containing a START domain at their C-terminus. The other two Rhoa GAPs are known as DLC1, DLC3 (Soccio & Breslow, 2003; Spagnoli & Brivanlou, 2006). In addition to the START domain, StarD13 contains a SAM domain at its N-terminus and a Rho GAP domain comprising its activity (Thorsell et al., 2011). The SAM domain has the ability to bind to other Sam domains, DNA, or RNA (Liao & Lo, 2008). StarD13 also have a potential in regulation apoptosis through its START domain, which targets the membrane of the mitochondria (Ng et al., 2006). Moreover, StarD13 contains at its

N-terminus a focal adhesion-targeting region (FAT) that localize StarD13 to the adhesion structures (Kawai et al., 2009).

Observations indicate that StarD13 is overexpressed in lower grade cancer that demonstrate decreased proliferation and growth such as in HCC (Ching et al., 2003). Additionally, in beast cancer StarD13 plays the role of a tumor suppressor that is consistent with previous findings. But it depicts a major role in promoting cell motility, which explains the increased expression of this particular Rho Gap in higher grade breast cancer compared to less malignant, lower grade breast cancer (Hanna et al., 2014, p. 13). These results were also consistent when StarD13 was studied in colon cancer. Overexpressing StarD13 lead to the decrease in cell proliferation. However, Knocking down StarD13 inhibited 2D motility and increased invasion of colon cancer cells (Nasrallah et al., 2014).

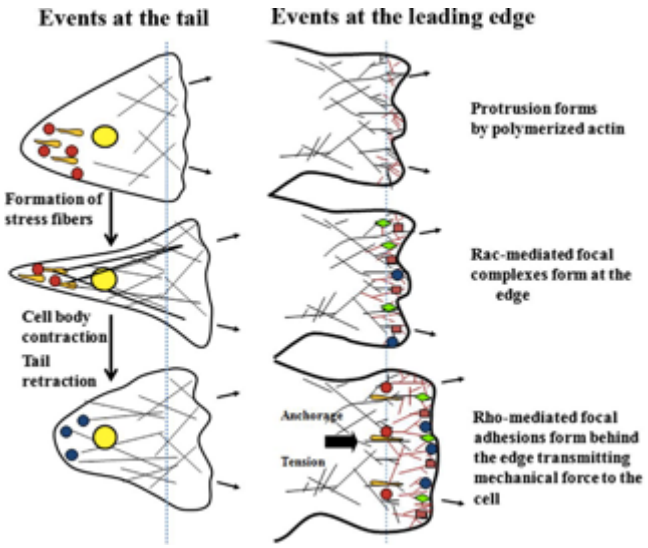

Figure 8: cell motility: RhoA activation cycle regulated by StarD13.
Source: (El-Sibai, unpublished)

1.7 Purpose of the Study

The aim of this study is to investigate the role of StarD13 in serous ovarian carcinoma SKOV3 in terms of cancer progression, proliferation, invasion, and motility.

Initially we aimed to examine the effect of StarD13 on cell proliferation, and if the results are consistent with the notion that StarD13 is a tumor suppressor. We accomplished this via knocking down StarD13 in different ovarian cancer cell lines such as (PA-1, CAOV3, and SKOV3) then cell cytotoxicity assay was performed.

Then, we aimed to elucidate the role of StarD13 in cell 2D and 3D motility. This was executed by wound healing assays, time lapses 'movies, and immunocytochemistry where we immunestained for proteins responsible for adhesion and invadopodia assembly, in addition to western blotting. StarD13 depletion drives the extensive assembly of invadopodia. So we wanted to research if the invadopodia is driven by the activation of Cdc42. Moreover, the depletion of StarD13 leads to the regression of 2D motility. Consequently, the study aspires to answer if this regression is due to the inactivation of Cdc42 or the deterioration of RhoA's ATP/GTP cycle.

Finally, the inspection whether StarD13 is an actual Rho GAP for RhoA and/or Cdc42 was completed via pull down assays.

The objective of this study in conclusion is to assure that in ovarian cancer StarD13 is a tumor suppressor, a Rho GAP for Cdc42, and it aids in cancer cell motility.

Chapter Two

Materials and methods

2.1 Cell culture

Ovarian serous carcinoma (SKOV3, CAOV3, PA-1) were obtained from ATCC, and were cultured in DMEM medium supplemented with 10% FBS and 100 U penicillin/streptomycin at 37°C and 5% CO2 in a humidified chamber.

2.2 Antibodies and reagents

The following primary antibodies were used in this study: Goat polyclonal anti-StarD13, mouse monoclonal anti-RhoA antibody, rabbit polyclonal anti-cdc42, mouse monoclonal anti- Rac1, rabbit polyclonal anti-Paxillin, rabbit polyclonal anti-Tks4, rabbit polyclonal anti-cortactin, rabbit monoclonal anti-WASP, rabbit rabbit polyclonal Arp2, rabbit polyclonal anti-beta actin were purchased from abcam (Abcam Inc., Cambridge, UK) and (Santa Cruz Inc., Delaware, CA, USA). Anti-rabbit and anti-mouse HRP-conjugated secondary antibodies were obtained from promega (Promega Co., Wisconsin). Fluorescent secondary antibodies (Alexa Fluor 488) were obtained from Invitrogen. For F-actin cytoskeleton visualization, cells were stained with Rhodamine-phalloidin (Invitrogen).

2.3 Cell transfection with siRNA

Flexi Tubes siRNA for StarD13 oligo3 and 8, RhoA oligo 1 and 6, Cdc42 oligo 4 and 7,and for Rac1 oligo 5 and 6 were obtained from Qiagen (Qiagen, USA). The cells were transfected with the siRNA at final concentration of 10 nM using Hiperfect (Qiagen, USA) according to the manufacturer's specifications. Control cells were transfected with siRNA sequences targeting GL2 Luciferase (Qiagen, USA). After 72 hours, protein levels in total cell lysates were analyzed by western blotting using the appropriate antibodies.

2.4 Western Immunoblotting

Whole cell lysates were prepared by scraping the cells with laemmli sample buffer (LSB) containing 4% SDS, 20% glycerol, 10% β mecraptoethanol, 0.004% bromophenol blue and 0.125M Tris HCL (pH 6.8). SDS-PAGE was carried out under standard conditions and proteins were blotted onto a PVDF membrane. The membranes were then blocked with 5% bovine serum albumin for 1 hour and then incubated overnight at 4°C with either primary antibody against StarD13 (Santa cruz, 1: 200 dilution), RhoA, Cdc42, Rac1 (abcam, 1:500 dilution), or actin (abcam, 1:2500). After the incubation with the primary antibody, the membranes were washed and incubated with secondary antibody at a concentration of 1:1000 for 1 hour at room temperature. The membranes were then washed, and the bands visualized by treating the membranes with western blotting chemiluminescent reagent ECL (GE Healthcare). The levels of protein expression were compared by densitometry using the ImageJ software.

2.5 Cell proliferation reagent (WST-1)

Cells were seeded in 96-well plates (growth area: 0.6 cm^2) at a concentration of 1×10^6 cells/ml. Depending on the experiment, cells were transfected with StarD13 siRNA with appropriate controls. Following treatment period, 10 μl of cell proliferation reagent (WST-1; Roche, Germany) was added to each well. The plates were incubated at in a humidified incubator (37˚C) in 95% air and 5% CO_2 for 2 h. WST-1 is a tetrazolium salt that on contact with metabolically active cells is cleaved to produce formazan dye by mitochondrial dehydrogenases. Quantitation of formazan is done colorimetrically at 450 nm. The absorbance of the each blank well was subtracted from the corresponding sample well. The results were normalized to the corresponding controls, and the percent of cell proliferation was reported.

2.6 Adhesion assay

96-well plates were coated with collagen using Collagen Solution, Type I from rat tail (Sigma) overnight at 37 °C then washed with washing buffer (0.1% BSA in DMEM). The plates were then blocked with 0.5% BSA in DMEM at 37 °C in a CO2 incubator for 1 hour. Washing the plates and chilling them on ice followed this. Meanwhile, the cells were trypsinized and counted to 4x105 cell/ml. 50 µl of cells were added in each well and incubated at 37°C in a CO2 incubator for 30 minutes. The plates were then shaken and washed 3 times. Cells were then fixed with 4% paraformaldehyde at room temperature for 10 minutes, washed, and stained with crystal violet (5 mg/ml in 2% ethanol) for 10 minutes. Following the staining with crystal violet, the plates were washed extensively with water, and left to dry completely. Crystal violet was solubilized by incubating the cells with 2% SDS for 30 minutes. The absorption of the plates was read at 550 nm using an ELISA reader.

2.7 Invasion Assay

Cells were transfected with control, and StarD13 then invasion assay was performed 48hrs following treatment period using the collagen-based invasion assay (Millipore) according to manufacturer's instructions. Briefly, 24hrs prior to assay, cells were starved with serum free medium. Cells were harvested, centrifuged and then re-suspended in quenching medium (without serum). Cells were then brought to a concentration of 1x106 cells/ml. In the meantime, inserts were pre-warmed with 300µl of serum free medium for 30min at room temperature. After rehydration, 250µl of media was removed from inserts and 250µl of cell suspension was added. Inserts were then placed in a 24-well plate, and 500µl of complete media (with 10% serum) was added to the lower wells. Plates were incubated for 24hrs at 37oC in a CO2 incubator. Following 48 hours of incubation period, inserts were stained for 20min at room temperature with 400µl of cell stain provided with the kit. Stain was then extracted with extraction buffer (also provided with the kit).100ul of extracted stain was then transferred to a 96-well plate suitable for colorimetric measurement using a plate reader. Optical Density was then measured at 560µm.

2.8 Wound healing

Cells were grown to confluence on culture plates and a wound was made in the monolayer with a sterile pipette tip. After wounding, the cells were washed twice with PBS to remove debris and new medium was added. Phase-contrast images of the wounded area were taken at 0 and 16 h after wounding. Wound widths were measured at 11 different points for each wound, and the average rate of wound closure was calculated in μm/h using the ImageJ software in pixels/h and then converted to μm/h by multiplying by the pixel size corresponding the objective used in these experiments.

2.9Motility assay

Cells were plated on a 35mm petri dish and transfected with si-Luciferase, si-StarD13. The assay was performed 72 hours after transfection. For motility analysis, cells were imaged in DMEM (10% FBS) media, buffered using HEPES and overlaid with mineral oil on a 37°C stage. Images were collected every 60 seconds for 2 hours using a 20X objective lens on Zeiss Observer Z1 microscope. The speed of cell movement was quantified using the ROI tracker plugin in the ImageJ software, which was used to calculate the total distance travelled by individual cells. The speed is then calculated by dividing this distance by the time (120 minutes) and reported in μm/min. The speed of at least 10 cells for each condition was calculated. The net distance travelled by the cell was calculated by measuring the distance travelled between the first and the last frame.

2.10 Immunocytochemistry

Cells were plated on glass coverslips on collagen with a final concentration of 50μg/mL, either plotted without treatment, or starved for 3 hrs and treated with EGF. Cells were fixed with 4% paraformaldehyde for 10 minutes at 37o, and permeabilized with 0.5% Triton-X 100 for 15 minutes on ice. For blocking, cells were incubated with 1% filtered BSA in PBS for 1 hour. Samples were then stained with primary antibodies overnight at 4 degrees and with fluorophore-conjugated secondary antibodies for 1 hour. Fluorescent images were taken using a 63X objective lens on Zeiss Observer Z1 microscope.

2.11 Pull-down assay

Cells were transfected with si-Luciferase and si-Cdc42, following treatment period, cells were lysed, and the pull-down assay performed using the

RhoA/Rac1/Cdc42 Activation Assay Combo Kit (Cell BioLabs) following the manufacturer's instructions. Briefly, cell lysates were incubated with GST-RBD (for RhoA) or GST-PAK (for Rac1/Cdc42) for 1 hour at 4 °C with gentle agitation. Then, the samples were centrifuged, and the pellet washed for several times. After the last wash, the pellets were resuspended with sample buffer and boiled for 5 minutes. GTP-RhoA and GTP-Rac1/Cdc42 were detected by western blotting using anti-RhoA, anti-Rac1 and anti-Cdc42 antibodies provided in the kit. Total proteins were collected prior to the incubation with GST beads and used as a loading control.

2.12 Live upshift assay

Cells were plated on a 35mm petri dish. Cells were then stimulated with EGF and imaged every 30 seconds up to 15 minutes in DMEM (10% FBS) media, buffered using HEPES and overlaid with mineral oil on a 37°C stage using a 63X objective lens on Zeiss Observer Z1 microscope. The area of the cells before and after stimulation was quantitated using image j software.

2.13Quantitation of focal adhesions

Image J was used to quantitate focal adhesions. Briefly, two main plugins were used to quantitate focal adhesions; these two plugins are CLAHE and Log3D. CLAHE enhances the local contrast of the image and Log3D filters the image based on user predefined parameters, which will allow us to detect and analyze focal adhesions (Horzum, Ozdil, & Pesen-Okvur, 2014).

Chapter Three

Results

3.1 Knocking down StarD13 using Si-RNA

At first, the knock down of StarD13 was established using small interfering RNA successfully, and the better oligonucleotide that resulted in enhanced knockdown was determined. Thus western blot was conducted to resolve the level of StarD13 expression after transfecting the cells with the control (Luciferase), and two oligonucleotides of StarD13 (oligo3, oligo8) in three different ovarian cancer cell lines (SKOV3, CAOV3, PA-1). (Figure9). The expression level of StarD13 using oligo 3 is decreased by approximately 80% compares to 75% decrease using oligo 8 in SKOV3 cell line. To eliminate inaccuracy due to loading if the lysate in western we used β actin as a loading control. Oligo 3 and 8 were also successful in depleting StarD13 in CAOV3 and PA-1 cell lines with oligo 8 showing more improved ability to knockdown StarD13. Consequently, we continued our experiments using oligo3 and oliogo8.

3.2 StarD13 is a tumor suppressor

Previous research established the function of StarD13 as a tumor suppressor in several cancers; therefore we wanted to study if previous findings are pertained in ovarian cancer. After establishing a successful depletion of StarD13 using the appropriate si-RNA oligonucleotides and transfecting for 72 hours, cell viability increased in SKOV3, CAOV3, and PA-1 upon knocking down StarD13, concluding that StarD13 is indeed a tumor suppressor in ovarian cancer (Figure 10).

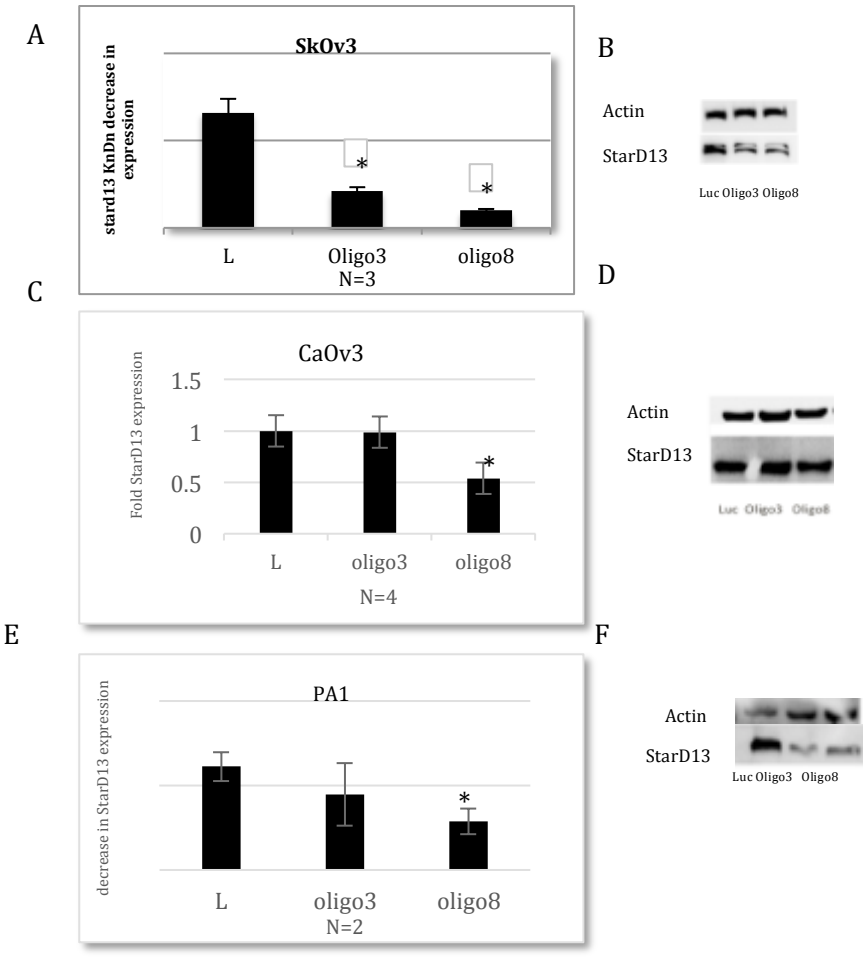

Figure 9: western immunoblotting to determine the expression of StarD13 in several ovarian cancer cell lines: Cell lines were transfected with control si-RNA, Oligo3 StarD13 si-RNA, and Oligo8 StarD13 si-RNA for 72 hrs. Knockdown of StarD13 is successful using si-RNA, which is evident by the decreased expression of StarD13 compared to the control (Luciferase). Western blot quantification showing the efficient knockdown when oligo3 is used in SKOV3 cell lines (A), and when oligo 8 is used in CAOV3 (C), PA-1 (E). Cells were lysed and immune blotted by western blot for Stard13, and Actin (loading control) in SKOV3 (B), CAOV3 (D), and PA-1 (F). Data are the mean -/+ SEM of three independent experiments.

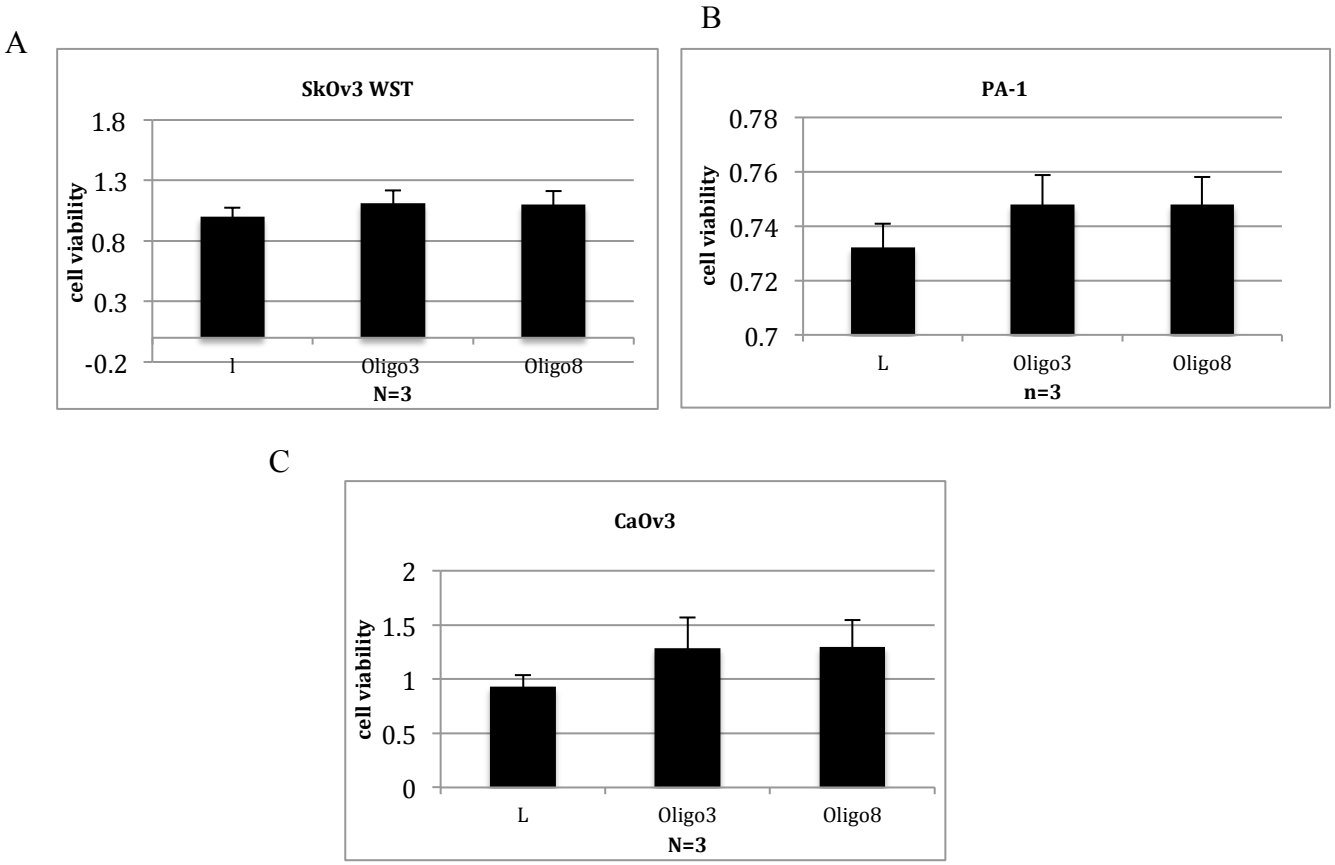

Figure 10: StarD13 decrease cell viability playing its role as a tumor suppressor: Cell proliferation was determined using WST-1 reagent. Cell viability of si-RNA-transfected cells was expressed as fold increase from control. (A) Skov3, (B) PA-1, and (C) CAOV3 cell lines depict an increase in cell viability upon knocking down StarD13 in comparison with cells transfected with luciferase (control). Data are the mean -/+ SEM of three independent experiments.

3.3 The role of StarD13 on ovarian cancer cell 2D motility:

3.3.1. StarD13 depletion decreases human ovarian cancer SKOV3 cell migration. However the knockdown of StarD13 increased cell migration in human ovarian cancer cell line CAOV3.

The cells were treated with StarD13 si-RNA oligonucleotides, in order to knockdown the protein and monitor its effect on cell motility. Wound-healing assay was conducted (Figure11). The rate at which the wound closes was quantified. Results showed that StarD13 is a positive regulator of cell motility in SKOV3 cell line as its knockdown decreased the rate at which the wound closes. However the depletion of StarD13 in CAOV3 cell line increased the rate of wound closure by approximately more than 50% (Figure 12, A, B).

Likewise, and in order to confirm the obtained results from the wound-healing assay, and with the same conditions applied, two dimensions time Lapse microscopy assay was conducted then the data for cell speed was quantitated using ImageJ. The results were consistent with the previous findings, and indicate that StarD13 is a positive regulator of cell motility in ovarian SKOV3 cell line. Conversely, it has a negative effect on cell motility in ovarian CAOV3 cell lines; cell speed increased from 0.03 μm/min to 0.04 μm/min upon knocking down StarD13 (Figure 12, C and D).

3.3.2 StarD13 knockdown decreases adhesion to collagen in human ovarian cancer SKOV3 cell line. However, the knockdown of StarD13 increased adhesion in CAOV3 ovarian cancer cell lines.

The formation of adhesion structures is a profound step in the motility cycle of the cell. Thus, the aim was to evaluate if the role of StarD13 in cell motility is due to its effect on focal points and adhesion structures formation. Subsequently, the adhesion assay was implemented on the two different cell lines (SKOV3, CAOV3), after transfecting the cell lines with the appropriate StarD13 siRNA oligonucleotides. The results revealed that upon knocking down StarD13 the adhesion increased by nearly 20% in SKOV3. While the adhesion decreased significantly by 51% in StarD13 depleted CAOV3 cell lines (Figure 13).

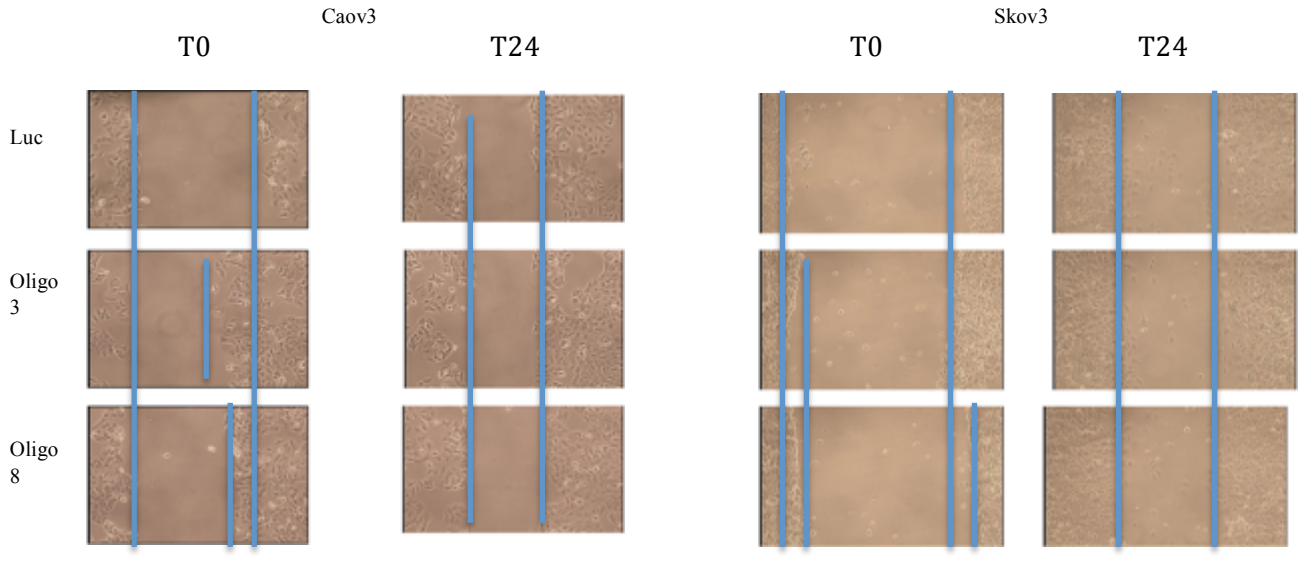

Figure11: wound healing assay of ovarian cancer cells SKOV3, and CAOV3 after transfection with si-RNA of StarD13 and control at time zero and after 24hours of forming the wound.

A

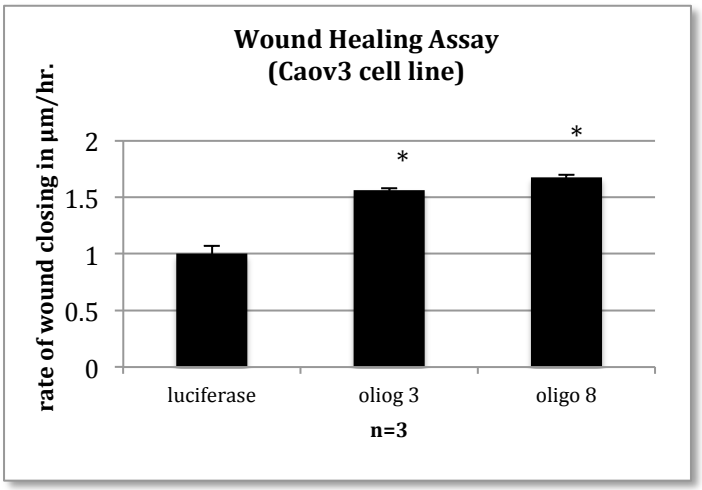

B

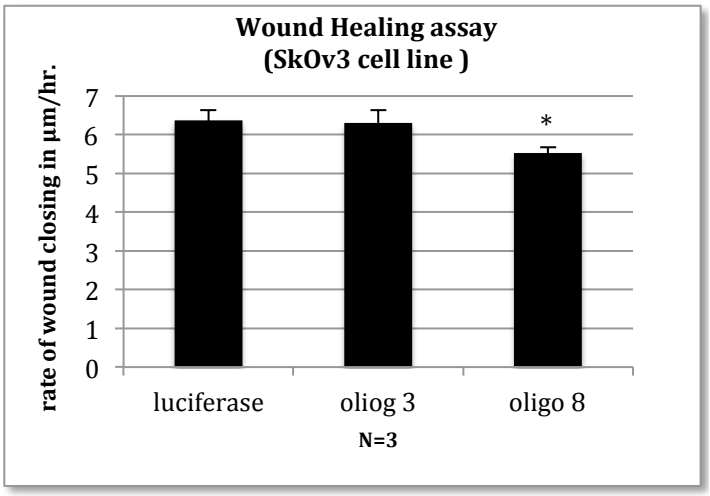

C

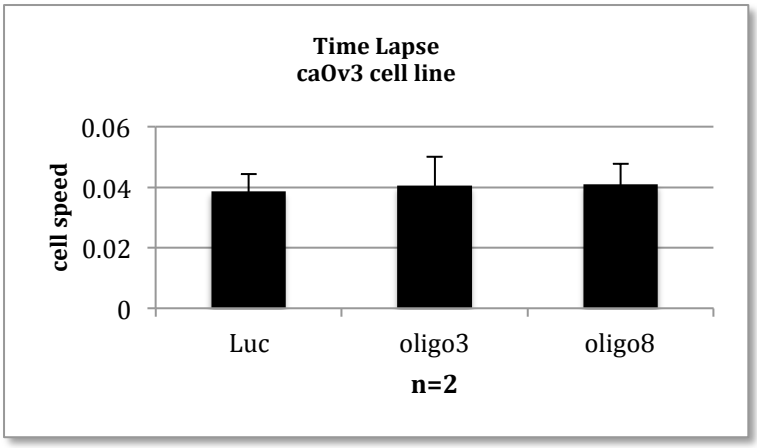

D

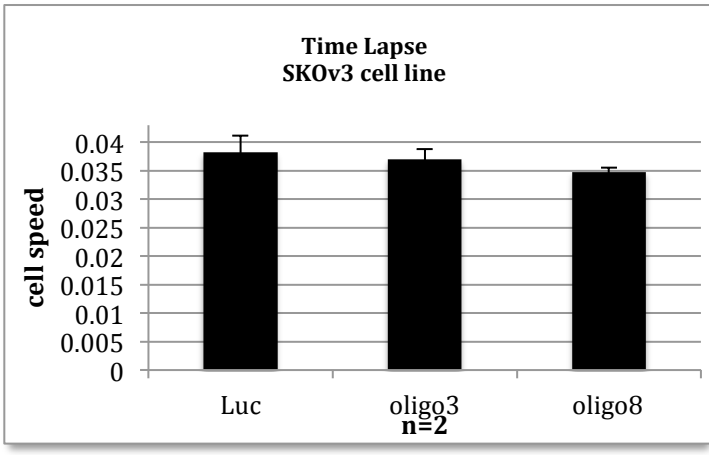

Figure 12: the effect of StarD13 Knockdown on cell motility: (A, B) depict the rate at which the wound closes in ovarian cancer cells transfected with StarD13 Si-RNA (CAOV3, and SKOV3 respectively). (C, D) portray the quantification of the net speed migration fold in CAOV3 and SKOV3 cell lines respectively, normalized to the control, of projected 120 frames from time lapse movies of cells with an overall duration of 2 hours displaying random cell motility in serum. Data are the mean -/+ SEM taken from 15 randomly selected cells.

3.4 StarD13 has a GAP activity for Cdc42 but not for RhoA

In order to comprehend the effect of knocking down StarD13 on the activity of RhoA and Cdc42, which was established using pull down assay in two ovarian cancer cell lines (SKOV3, CAOV3). SKOV3 Cells transfected with StarD13 Si-RNA showed an approximately 80% increase in the level of expression of active Cdc42 (GTP- bound Cdc42). However the active RhoA expression levels decrease slightly upon knocking down StarD13. Indicating that in SKOV3 cell lines, which are a serous adenocarcinoma, StarD13 is a Cdc42 Rho GAP but it doesn't affect the activity of RhoA. Similarly, CAOV3 cell line when depleted from StarD13 using Si-RNA, results in two folds increase in the expression levels of active Cdc42, and the level of active RhoA is decreased. Hence, the results are consistent in these two cell lines (Figure 14).

3.5 the effect of StarD13 depletion on the formation of focal adhesion

In order to corroborate the cell adhesion assay results in ovarian serous carcinoma SKOV3, the formation of focal adhesions must be studied, which are the mediators of the adhesion process. After knocking down Rac1, Cdc42 or both proteins, in order to confirm the pull down assay results, which indicate that StarD13's effect on cell adhesion and motility is driven by the deactivation of Cdc42 and regardless of RhoA. Hence, ICC was conducted where Paxillin was stained. In control we see the point contacts and the FA. In Rac1 depletion both decreased. In the Cdc42 depletion both decreased to a later extent compared to Rac1 knockdown. In the Cdc42/RAC the number of focal adhesions are more compared to Cdc42 knockdown but less than the control (figure 14), which indicates that StarD13 in

Skov3 cells deactivate Cdc42 which in turn deactivate Rac1. Consequently, disrupting the activation /deactivation cycle of Rac1/RhoA, as we know that Rac1 is the antagonist of RhoA, and Rac1 is needed for the focal point formation so it is needed to be activated first, then RhoA activation would lead to the maturation of the focal points into focal adhesions. But When StarD13 is present in SKOV3 cell line, Cdc42 and Rac1 is inactivated hence the focal points aren't formed which in turn reduces the cells ability to adhere to the ECM facilitating the cells movement.

(Figure15).

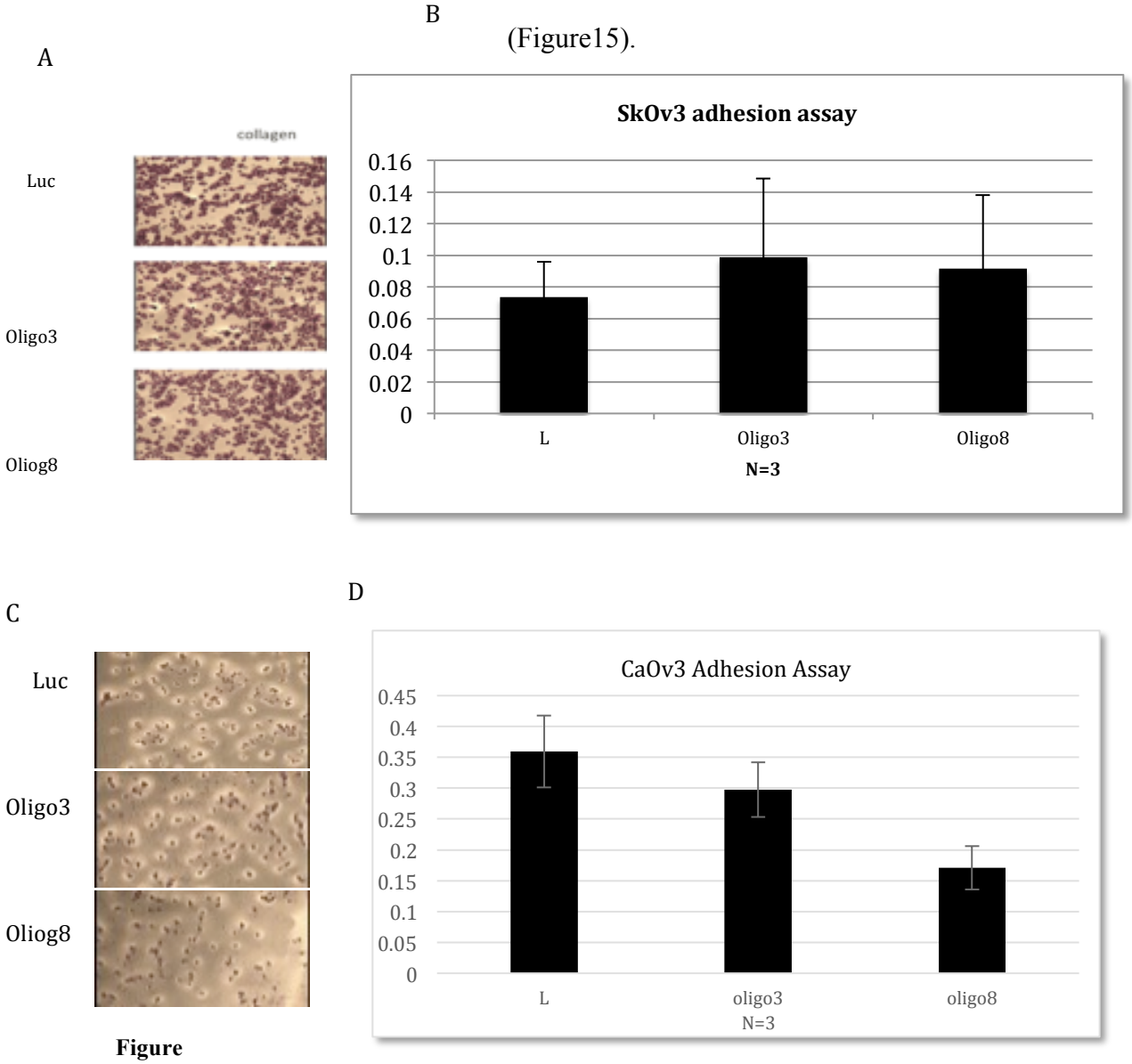

Figure 13: the effect of StarD13 knockdown on cell adhesion to collagen: A) Representative micrographs of SKOV3 cells transfected with si-Luciferase (Upper lane), si-StarD13 oligo3 (middle lane), si-StarD13 oligo8 (lower lane), fixed and stained with crystal violet (as described in methods. B) Quantitation of solubilized Crystal violet from SKOV3 plates and the absorption of the plates were measured at 550 nm using an ELISA plate reader. Data are

measured in fold change of adhesion normalized to the control. C) Representative micrographs of CAOV3 cells transfected with si-Luciferase (Upper lane), si-StarD13 oligo 3 (middle lane), si-StarD13 oligo 8 (lower lane), fixed and stained with crystal violet (as described in methods). D) Quantitation of solubilized Crystal violet from CAOV3 plates and the absorption of the plates at 550 nm using an ELISA plate reader. Data are measured in fold change of adhesion normalized to the control. Data are the mean -/+ SEM from 3 independent experiments.

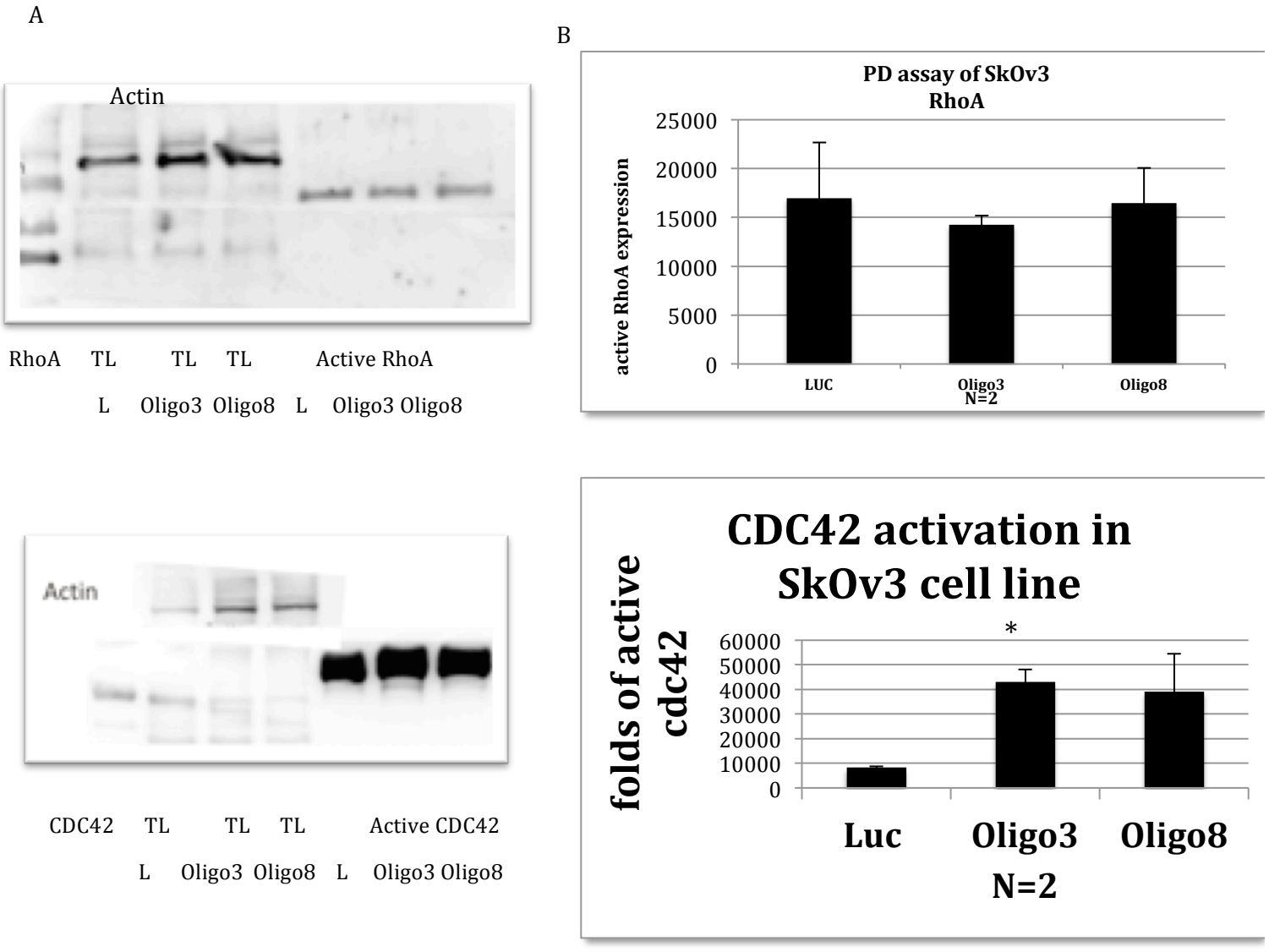

Figure 14: StarD13 is a Cdc42 GAP but not a GAP for RhoA in SKOV3/CAOV3 cell lines: SKOV3 /CAOV3 cells were lysed after being transfected with StarD13 Si-RNA for 72 hrs. Afterwards the lysate was incubated with either GST-RBD to pull down active RhoA (A, G), or with GST-PAK to pull down active Cdc42 (C, E). (A, G and C, E) GTP-RhoA and GTP- Cdc42 were detected by western blotting using anti RhoA and anti Cdc42. Total proteins collected prior to the incubation with GST beads were used as a loading control. (B, H and D, F) Active RhoA and active Cdc42 bands were quantitated respectively using image J and normalized to the amount of total lysate that in turn were normalized to the amount of actin to eliminate further loading errors

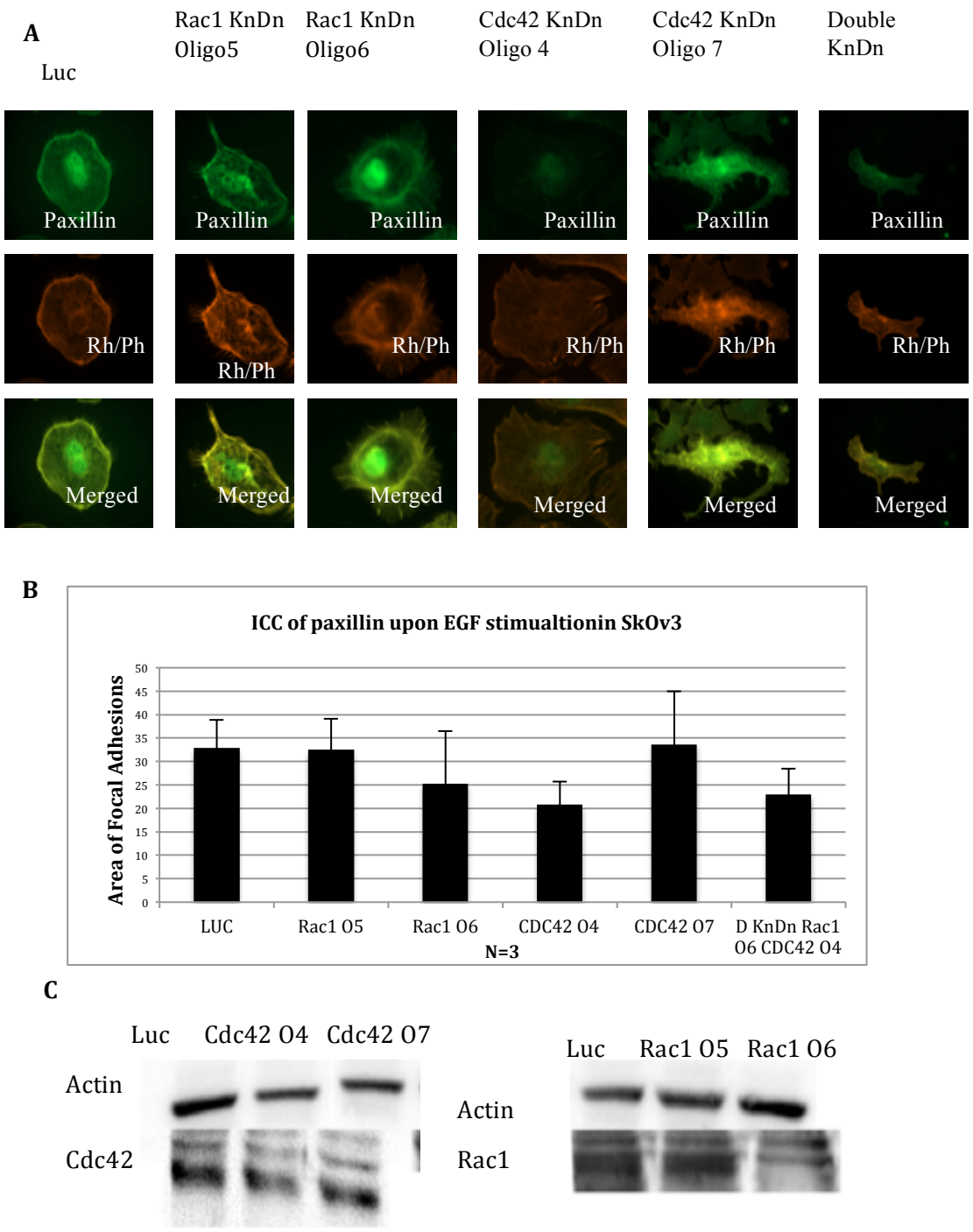

Figure 15: FigureStarD13 knockdown effect on the formation of focal adhesion. A) Representative micrographs of (SKOV3) transfected with si-luciferase (first lane), si-Rac1 oligo5 (second lane), si-Rac1 oligo6 (third lane), si-Cdc42 oligo4 (fourth lane), si-Cdc42 oligo7 (fifth lane), and double knockdown of Cdc42/Rac1 (sixth lane), which were fixed and stained with anti-Paxillin. Cells were imaged using a 60x objective. B) Quantitation of number of focal adhesions (upon Rac1, Cdc42, and double Rac1/Cdc42 knockdowns). Data are the mean -/+ SEM from 3 independent experiments. C) SKOV3 cells were transfected with control siRNA, Cdc42 siRNA (left), Rac1 siRNA (right) for 72 hours to confirm that a successful knockdown occurred.

3.6 StarD13 has a negative effect on the formation of ovarian cancer cells ruffles and protrusions

Based on the previous, Cdc42/Rac1 regulate the formation of focal adhesions in SKOV3 ovarian cancer cells. Moreover, based on previous research, (Hanna et al., 2014) concluded that stimulated protrusions in breast cancer cells requires the activity of Cdc42. Accordingly the question at hand now is if Cdc42 drives the regulation and formation of actin structures in ovarian cancer SKOV3 cell. Thus a lamellipodia response in serous ovarian carcinoma SKOV3 cells was established, in order to observe the effect of StarD13 knockdown on cell morphology and size. Thus, Epidermal Growth factor (EGF) was used to stimulate with and detect an increase in protrusion under live imaging

3.6.1 EGF stimulation had no measurable effect on the size of SKOV3 cells but clear increase in the cell ruffling was observed.

Accordingly, live upshift assay was performed where SKOV3 cells were transfected with si-StarD13 and si-Cdc42 and with both oligonucleotides. Then live imaged for 20 minutes, and stimulated with EGF after 10 minutes of imaging. Afterwards the size of cells was quantitated using ImageJ. The results showed no difference whatsoever on the cells size before or after the EGF stimulation. However we observed an increased in cell ruffling (figure 16, A). Nevertheless, quantitating the ruffling form the live upshift movies wasn't applicable. Therefore, immunocytochemistry assay was executed with the same transfection conditions and SKOV3 cells were stimulated with EGF for 10 minutes then fixed and stained for

Arp2 the protein that drives cell ruffles and the formation of de novo actin filaments.

In addition to staining the cells with Rhodamine/Phalloidin.

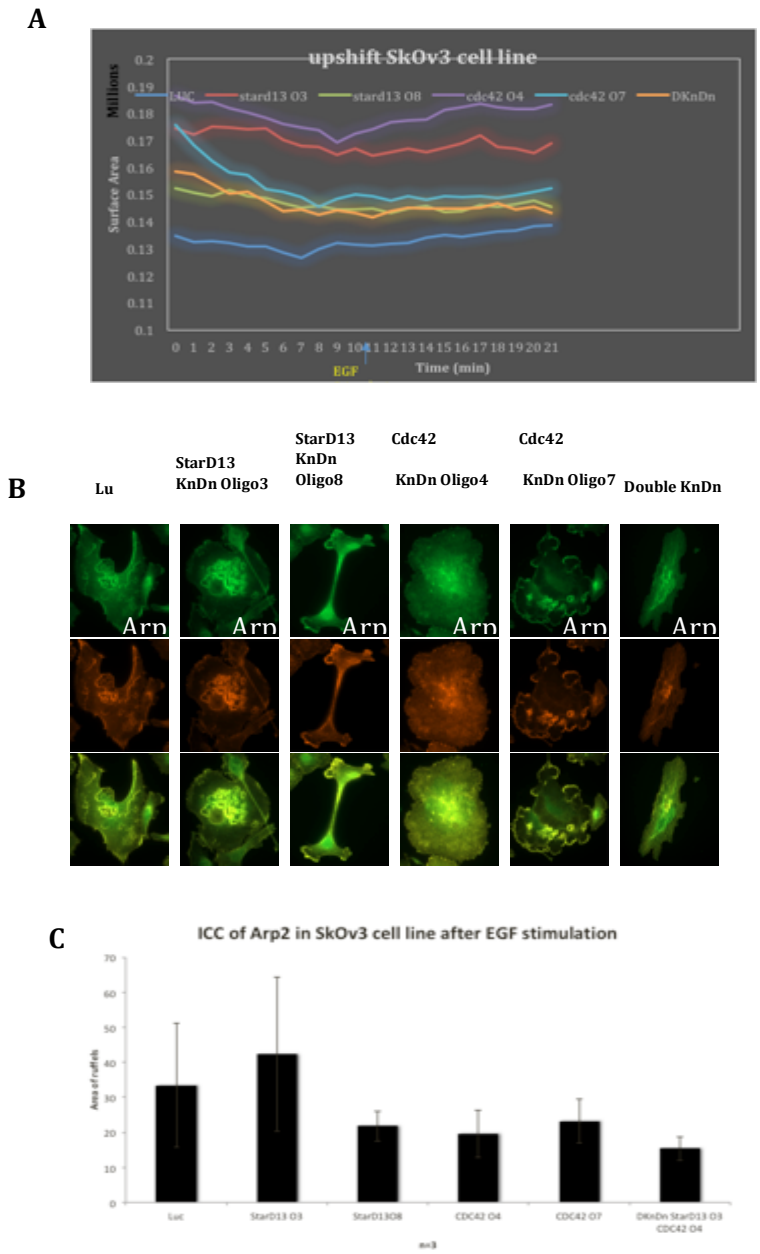

Figure 16: StarD13 negatively regulate EGF stimulated protrusions in SKOV3 cells by deactivating Cdc42: A) quantitation of SKOV3 cell sizes after performing a live upshift assay were at the minute 10 cells were stimulated with EGF. B) Represents a micrograph where SKOV3 cells were transfected with si-Luc, si-StarD13 oligo3, si-StarD13 oligo8, si-Cdc42 oligo4, si-Cdc42 oligo7, and double knockdown of StarD13/Cdc42 (respectively from left to right). Then cells were stimulated with EGF for 10 min, then fixed and stained for Arp2 (upper panel), Rhodamine/Phalloidin (middle panel), and micrographs of merged signals (lower panel). C) Quantitation of the area of ruffles using ImageJ (upon StarD13, Cdc42, and double StarD13/Cdc42 knockdowns). Data are the mean -/+ SEM from 3 independent experiments.

The results of the immunocytochemistry performed depict a 20% increase in ruffles area upon the knocking down of StarD13. Whereas an approximate 57% decrease in the area of ruffles upon depleting Cdc42. Furthermore, 45% decrease of ruffles area was detected upon knocking down both StarD13 and Cdc42. These results are consistent with the notion that Cdc42 drives the formation of actin structures and membrane ruffles through the regulation of StarD13 the Cdc42 Rho GAP (figure 16, B and C).

3.7 StarD13 is responsible for cell invasion regression in serous ovarian carcinoma SKOV3 cells, and the depletion of StarD13 lead to the increase in the number of invadopodia assembled.

3.7.1 StarD13 depletion promoted the invasion of SKOV3 cells

This study confirmed the Role of StarD13 in 2D motility, cellular adhesion, and the formation of focal adhesion. Succeeding, the next step was to study the role of StarD13 in cellular invasion (3D motility). Thus, a collagen based invasion assay was conducted in vitro where FBS was used as a cellular chemo attractant. SKOV3 cells were transfected with si-StarD13, and after 72 hours of incubation, cells were plated in a trans well membrane in a serum free media. In addition to an appropriate negative control, in which trans wells were filled with a serum free media only. The depletion of StarD13 promoted cellular invasion by around 26% (figure 17, A and B).

The increase in cellular invasion was due to the encouraged activation of Cdc42 upon StarD13 depletion. In order to confirm this hypothesis multiple immunocytochemistry assays were carried out, where we stained for the proteins responsible for the assembly of invadopodia structures. Accordingly ovarian SKOV3 cells were transfected with si-StarD13, si-Cdc42, and both, then cells were incubated for 72 hours. Next, cells were fixed and stained for Cortactin, Tks4, and Wasp.

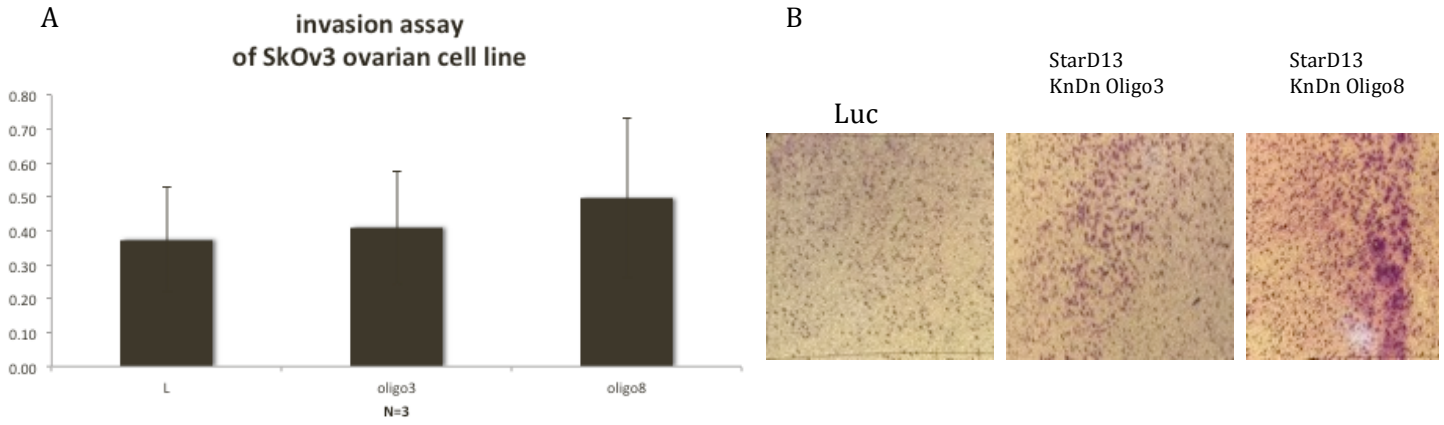

Figure 17: StarD13 depletion in SKOV3 cells promotes cellular invasion: SKOV3 cells were transfected with si-luciferase, and si-StarD13. The cells were incubated 72 hours in a trans well, the cells that invaded the collagen membrane in the direction of the chemo attractant FBS were extracted and stained then measured at 560 nm. A) Quantitation of the optical density for SKOV3 cellular invasion upon StarD13 knockdown. Data are the mean of +/- SEM of 3 independent experiments for each cell line. B) Micrographs of SKOV3 cells invading the collagen membrane.

3.7.2 StarD13 depletion promoted the assembly of Cdc42 induced invadopodia

When the study confirmed that StarD13 is indeed a tumor suppressor, which regresses the invasion in ovarian SKOV3 cell line, the study aimed to investigate the regulation and maturation of invadopodia; whether it is regulated due to the fact that StarD13 is a Rho GAP for Cdc42. Moreover, upon the depletion of StarD13, and consequently due to the activation of Cdc42, the assembly proteins are enabled.

The localization of the assembly proteins (Cortactin, Tks4, and Wasp) at the invading protrusions indicated the maturation of the invadopodia. Therefore, several immunocytochemistry assays were carried out where Skov3 cells were transfected with StarD13 and Cdc42 si-oligonucleotides, in addition to the control (si-luciferase). After 72 hours of incubation with the small interfering RNA, SKOV3 cells were fixed and then stained for Cortactin (Figure 18), Tks4 (Figure 19), and Wasp (Figure 20).

The results indicate that upon the depletion of StarD13, the number of invadopodia increased with the increased localization of Cortactin at the invading protrusions by approximately 44 %. But the knockings down of Cdc42 leads to a significant decrease in the number of invadopodia assembled by nearly 70%, the double knockdown of StarD13/Cdc42 depicts a 60% decrease in the number of assembled invadopodia (Figure 18).

Likewise, the number of invadopodia assembled after staining SKOV3 cells with Tks4 decreased by 20% upon Cdc42 knockdown. Whereas upon StarD13 knockdown the number increased by 36%. While 14% increase in the number of invadopodia assembly is observed after the depletion of both StarD13 and Cdc42, which indicates that more Tks4 were recruited to the invadopodia structures

(Figure19). Similarly, staining for Wasp denotes the significant regression in the number of invadopodia assembled upon knocking down Cdc42 (67% decrease), also upon knocking down both StarD13 and Cdc42 (48% decrease). While the invadopodia accounted for approximately 95% increased in number when StarD13 is depleted (Figure20).

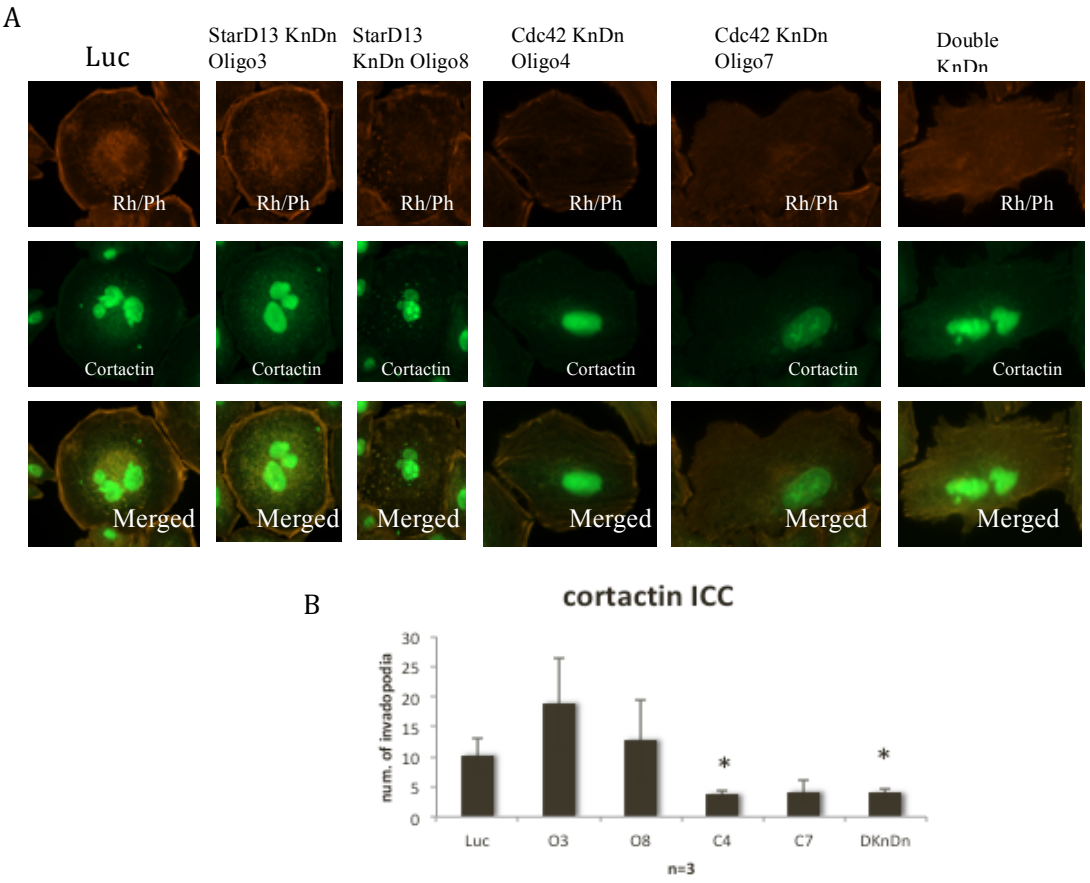

Figure 18: Immunocytochemistry of Cotrtactin to depict the number of invadopodia upon the depletion of StarD13 in ovarian cancer cell line SKOV3: A) monograph of SKOV3 cell after transfecting with si-luciferase, si-StarD13 oligo3, si-StarD13 oligo8, si-Cdc42 oligo4, si-Cdc42 oligo7, and double knockdown of StarD13/Cdc42 (from left to right respectively). After 72 hours of incubation cells were fixed and stained for Rhodamine/Phalloidin (upper panel), Cortactin (middle panel), and both signals merged (lower panel). B) The number of invadopodia formed was quantitated via ImageJ. Data are the mean of +/- SEM of 3 independent experiments for each cell line.

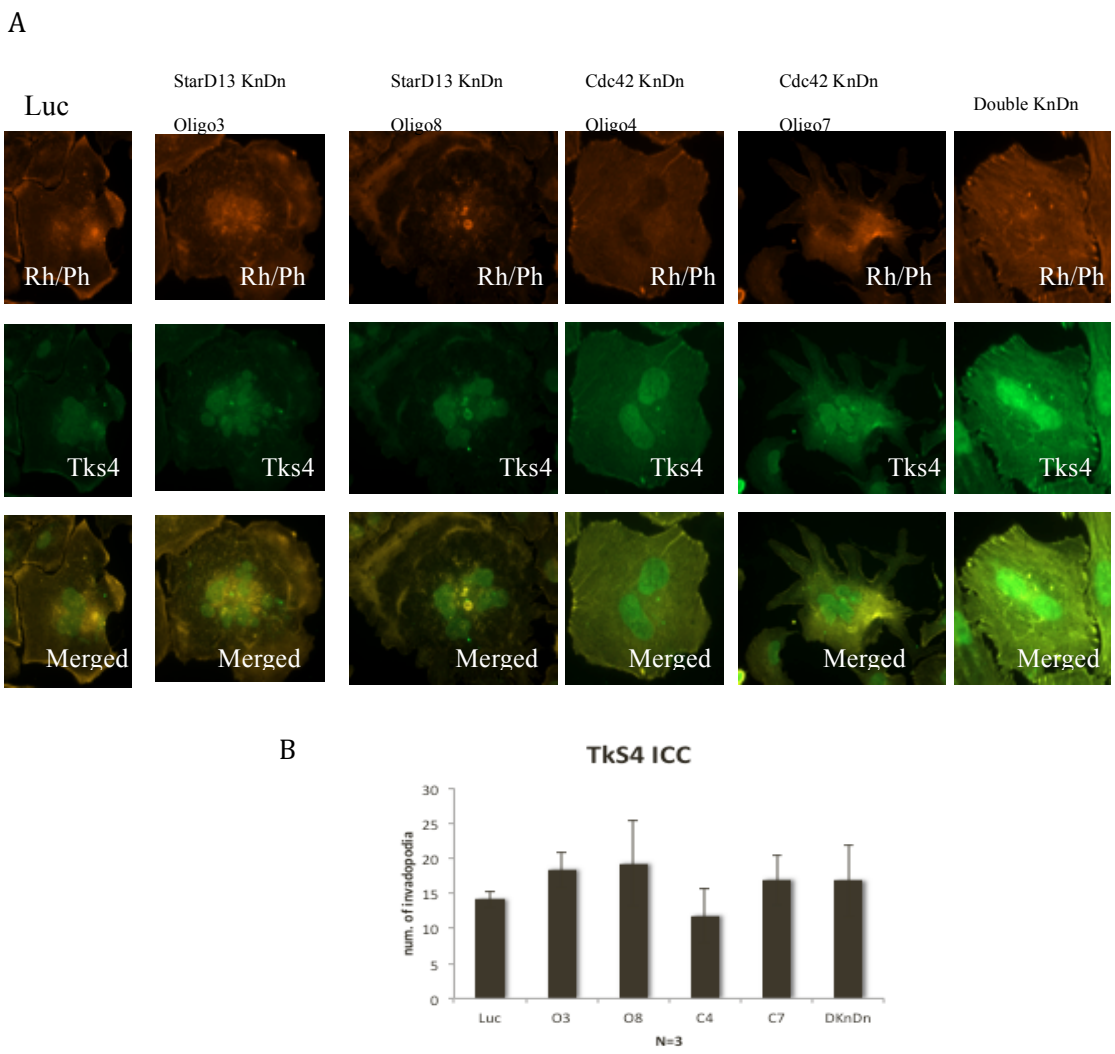

Figure 19: Immunocytochemistry of Tks4 to depict the number of invadopodia upon the depletion of StarD13 in ovarian cancer cell line SKOV3: A) monograph of SKOV3 cell after transfecting with si-luciferase, si-StarD13 oligo3, si-StarD13 oligo8, si-Cdc42 oligo4, si-Cdc42 oligo7, and double knockdown of StarD13/Cdc42 (from left to right respectively). After 72 hours of incubation cells were fixed and stained for Rhodamine/Phalloidin (upper panel), Tks4 (middle panel), and both signals merged (lower panel). B) The number of invadopodia formed was quantitated via ImageJ. Data are the mean of +/- SEM of 3 independent experiments for each cell line.

A

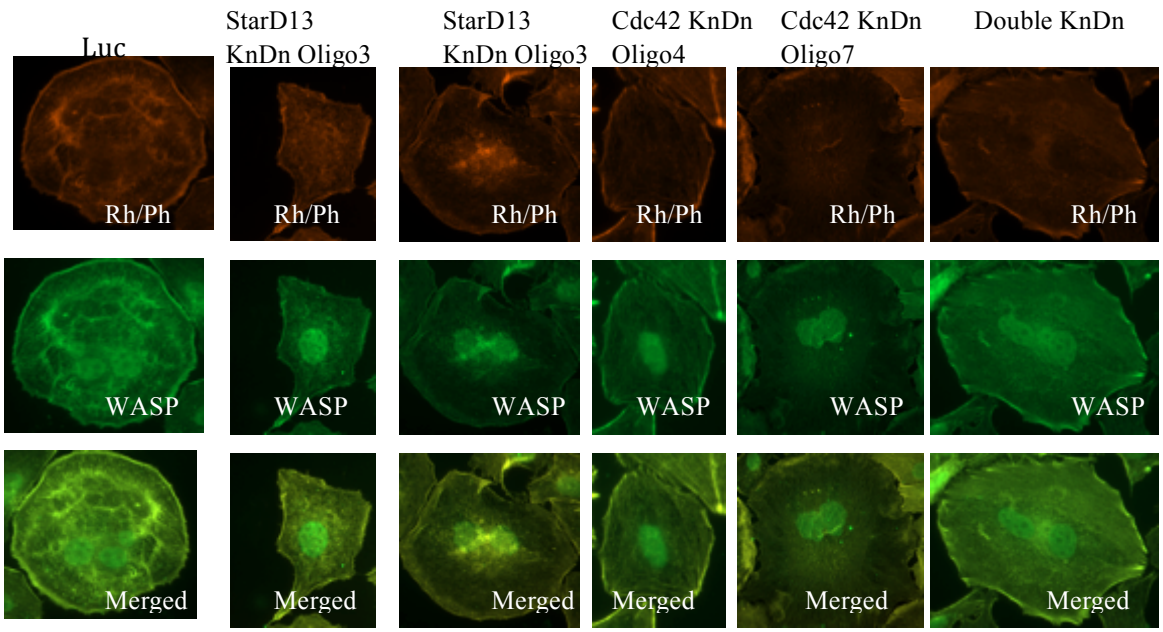

B

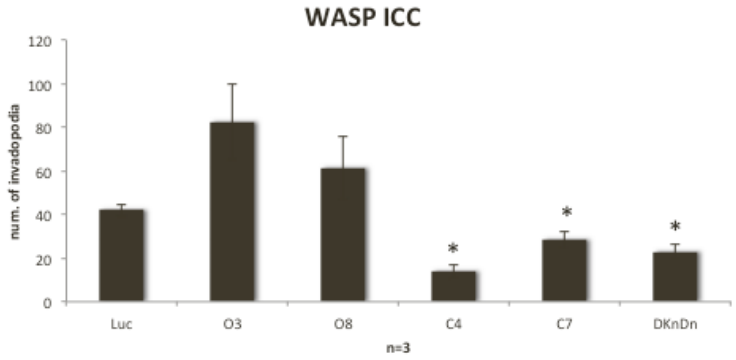

Figure 20: Immunocytochemistry of Wasp to depict the number of invadopodia upon the depletion of StarD13 in ovarian cancer cell line SKOV3: A) monograph of SKOV3 cell after transfecting with si-luciferase, si-StarD13 oligo3, si-StarD13 oligo8, si-Cdc42 oligo4, si-Cdc42 oligo7, and double knockdown of StarD13/Cdc42 (from left to right respectively). After 72 hours of incubation cells were fixed and stained for Rhodamine/Phalloidin (upper panel), Wasp (middle panel), and both signals merged (lower panel). B) The number of invadopodia formed was quantitated via ImageJ. Data are the mean of +/- SEM of 3 independent experiments for each cell line.

Chapter Four
Discussion

Ovarian cancer is composed of a pool of neoplasms, each with a specific characteristics and prognosis. Which entitle the cancer to be a heterogeneous disease. The heterogeneity of ovarian cancer is an essential source of treatment failure. Thus, Countless efforts have been made in order to identify each neoplasm, its signaling pathways that lead to malignancy, and prospective biomarkers for therapeutic purposes (Kossaï, Leary, Scoazec, & Genestie, 2018). Based on a previous research conducted at El-sibai's lab StarD13 was found to be a tumor suppressor in astrocytoma, breast, hepatocellular carcinoma, and colorectal cancer. StarD13 suppresses tumor growth by arresting the cell cycle instead of affecting the apoptosis pathways in order to suppress. Nevertheless, StarD13 is a positive regulator of cell motility via the cycling of RhoA/Rac1. Furthermore, StarD13 is found to be less expressed in cancerous tissue compared to normal tissue. However, higher-grade cancer expresses higher levels of StarD13 compared to lower grade-cancer. Accordingly depicting the importance of StarD13 in cell motility as it is required by the cell to increase 2D motility via regulating RhoA and Cdc42 (Ching et al., 2003; El-Sitt et al., 2012, p. 13; Hanna et al., 2014, p. 13; Khalil et al., 2014, p. 13; Nasrallah et al., 2014, p. 13)

Primarily, we made certain that the attenuation of StarD13 via si-RNA was conducted successfully using the most suitable oligonucleotides. Then we aimed to certify the role of StarD13 as a tumor suppressor in ovarian cancer. We conducted a cytotoxicity assay, where three different ovarian cell lines were depleted form StarD13. The silencing of StarD13 using small interfering RNA, increased cellular viability across the three ovarian cell lines. Which indicated the persistent role of StarD13 as a tumor suppressor in ovarian cancer. Then, we intended to confirm the role of StarD13 as a Rho GAP for Cdc42 and RhoA. We implemented Pull Down assay after silencing StarD13 to monitor the outcome on the activation levels of Cdc42 and RhoA in CAOV3 and SKOV3. The results indicated that StarD13 is a CDC42 Rho GAP. Still, no significant effect on the activation of RhoA was observed. Hence further research must be executed to confirm the previous. Nonetheless, we hypothesized that in ovarian cancer StarD13 is a tumor suppressor and a Cdc42 Rho GAP.

Afterwards, we wanted to study the role of StarD13 on cell 2D motility and adhesion. Cell motility assay and wound healing assay were applied after knocking down StarD13 in SKOV3 and CAOV3 cell lines. The silencing of StarD13 in SKOV3 cell lines led to decrease in cell speed and in the rate of wound closure. The opposite was obtained for the CAOV3 cell lines. From these findings, StarD13 is a positive regulator of cell motility in higher grade SKOV3 cell lines but it negatively regulate the 2D motility in lower grade CAOV3 cell lines. We suspected that these results were consistent with the notion that StarD13 regulates cell motility via regulating the adhesion. Indeed, the knockdown of StarD13 increased adhesion to collagen-based membrane in SKOV3, but decrease the adhesion ability in CAOV3 cell line, after running an adhesion assay.

StarD13 is found localize to the focal adhesions in astrocytoma along with RhoA. Furthermore, RhoA and Rac1 are antagonists in their regulatory roles (Khalil et al., 2014). Furthermore, (Hanna et al., 2014) showed that novel EGF stimulated protrusion formed due to the activation of Cdc42. Hence, we wanted to inspect the effect of StarD13 on focal adhesions, and the underlying method behind promoting cellular motility. Immunocytochemistry was conducted on SKOV3 cell line after silencing Rac1, and CDC42 or both after stimulating the cells with EGF, in order to verify that the focal adhesions formed are Rac/ cdc42 dependent regardless of the direct effect of RhoA. And we immunostained for Paxillin, the protein that regulates the formation and maturation of focal adhesions, we found that upon Rac1 depletion a slight decrease in focal adhesions area resulted. However the noteworthy decrease in focal adhesions area was due to Cdc42 depletion. Concluding that adhesive protrusions are Cdc42 regulated via the StarD13 GAP regardless of RhoA activation. Thereupon, we hypothesized that StarD13 drives cellular 2D motility via the deactivation of Cdc42, which in turn deactivate Rac1. Hence focal pointes driven by the activation of Rac1 cannot be formed, and the activation/deactivation cycle of Rac1/RhoA is disrupted, which in turn lessen the adhesive ability of the cells facilitating the cells movement.

To strengthen the previous results we studied the EGF stimulated membrane ruffling and the formation of protrusions via live upshift assay to check whether it is Cdc42-driven protrusions or not. We observed an increase in cell ruffles when StarD13 in knocked down while a decrease when Cdc42 is knocked down. Unfortunately, we could not quantitate the ruffles formed form the live upshift movies. Therefore, we conducted an immunocytochemistry where we depleted SKOV3 cells from StarD13, Cdc42, or both, and then we stained for Arp2, which

drives the actin polymerization to form the ruffles. The results from the immunostaining are consistent with the live upshift observations. We came to the conclusion that novel actin filaments and ruffles in SKOV3 are stimulated and regulated by the effect of StarD13 on the activation level of Cdc42.

Subsequently, we targeted the role of StarD13 in cellular invasion and 3D motility to be further examined. After we established the role of StarD13 on 2D cellular motility. We know from previous results that Cdc42 promotes the assembly of invading protrusions, and localize to the site of invadopodia assembly (Fortin Ensign, Mathews, Symons, Berens, & Tran, 2013).

Thus, we assessed the effect of StarD13 knockdown on cell invasion by performing a cellular invasion assay, which reflects the metastatic abilities of the cells studied. The depletion of StarD13 in SKOV3 increased the cellular invasion. Furthermore, to confirm our hypothesis, which indicates that StarD13 regulate 2D and 3D motility via Cdc42 regulation, we executed an additional immunocytochemistry, where SKOV3 cells were depleted from Cdc42 and StarD13, or both, and the cells where immunostained for the proteins that reflects the maturity of the invadopodia assembles (Cortactin, Tks4, Wasp). Knocking down Cdc42 decreased dramatically the number of the invadopodia assembled. On the contrary to StarD13 depletion in SKOV3, where the number of invadopodia quantitated was increased.

Chapter Five

Conclusion

This research aimed to explain the role of StarD13 on ovarian cancer cell progression, motility and invasion. We showed that starD13 is indeed a tumor suppressor in ovarian cancer, a Cdc42 Rho GAP that positively regulates 2D motility. However, StarD13 negatively regulates 3D motility.

StarD13's effect on the formation of focal adhesions, cell ruffles, and invadopodia is indispensable. StarD13 promotes the hydrolysis of GTP, in the active GTP-bound from of Cdc42, to GDP in order to inactivate Cdc42, which in turn inactivate Rac1, RhoA antagonist. Hereafter, disrupting the cycling of Rac1 and RhoA, and the focal points formed are not able to mature into focal adhesions so the cell would de-adhere and move. The results were coherent with our hypothesis, and with previous research conducted on other cancer types. Definitely, RhoA is responsible for the maturation of focal complexes and work antagonistically with rac1 to cycle the adhesion and de-adhesion of the cells rear and leading edge to drive the 2D migration.

Cdc42 has a crucial role in the assembly and maturation of invadopodia and protrusion structures, which is regulated by StarD13. The inactivation of Cdc42 by StarD13 promotes the inactivation of the proteins responsible for the assembly of invadopodia. Hence, StarD13 downgrade the 3D migration and invasiveness of ovarian SKOV3 cell line.

StarD13 is a tumor suppressor that promotes the migration of ovarian cancer

cells via regulating the activation of Cdc42.

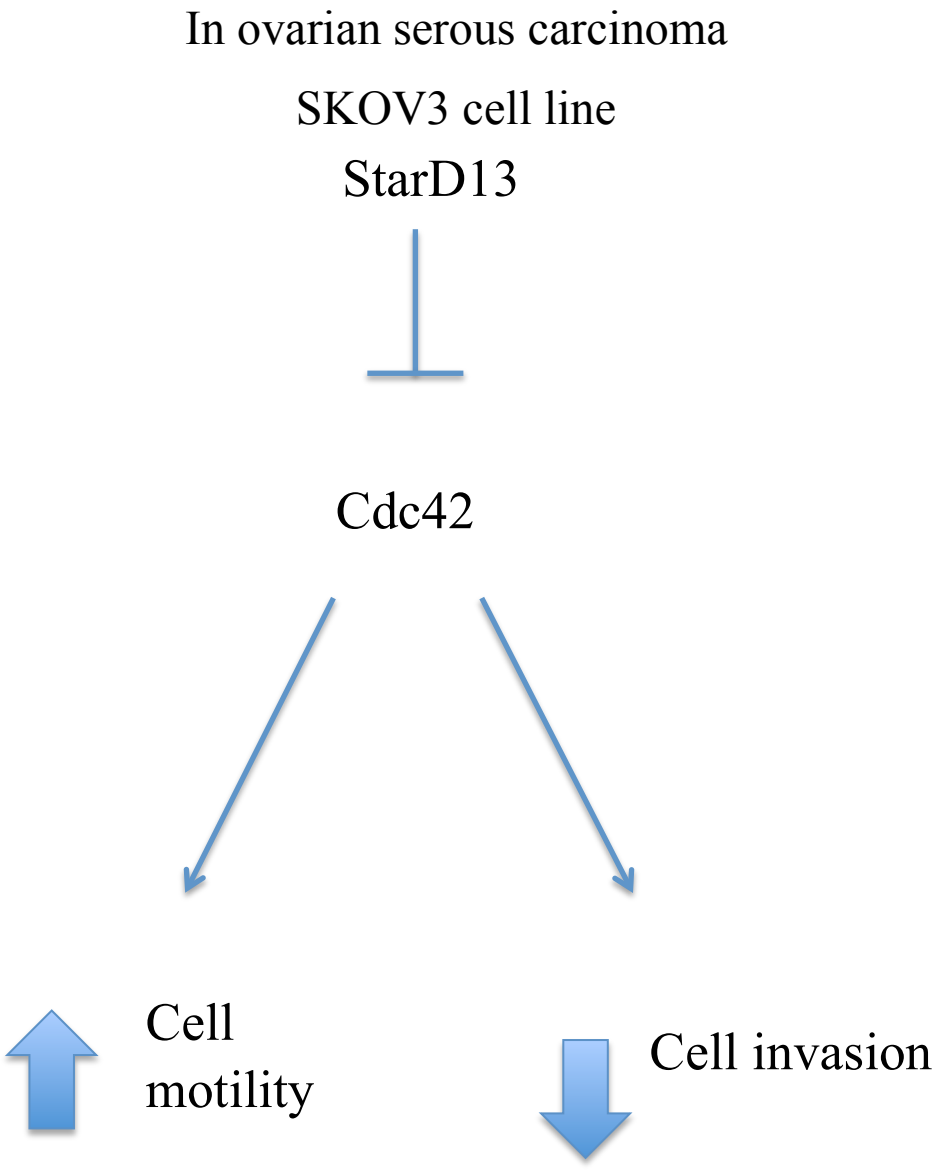

Figure21: the role of StarD13 in SKOV3 Ovarian Cancer

Bibliography

Akin, O., Sala, E., Moskowitz, C. S., Ishill, N., Soslow, R. A., Chi, D. S., & Hricak, H. (2008). Perihepatic metastases from ovarian cancer: sensitivity and specificity of CT for the detection of metastases with and those without liver parenchymal invasion. *Radiology*, *248*(2), 511–517. https://doi.org/10.1148/radiol.2482070371

Alblazi, K. M. O., & Siar, C. H. (2015). Cellular protrusions--lamellipodia, filopodia, invadopodia and podosomes--and their roles in progression of orofacial tumours: current understanding. *Asian Pacific Journal of Cancer Prevention: APJCP*, *16*(6), 2187–2191.

Ananthakrishnan, R., & Ehrlicher, A. (2007). The forces behind cell movement. *International Journal of Biological Sciences*, *3*(5), 303–317.

Bailly, M., & Condeelis, J. (2002). Cell motility: insights from the backstage. *Nature Cell Biology*, *4*(12), E292-294. https://doi.org/10.1038/ncb1202-e292

Beaty, B. T., & Condeelis, J. (2014a). Digging a little deeper: the stages of invadopodium formation and maturation. *European Journal of Cell Biology*, *93*(0), 438–444. https://doi.org/10.1016/j.ejcb.2014.07.003

Beaty, B. T., & Condeelis, J. (2014b). Digging a little deeper: the stages of invadopodium formation and maturation. *European Journal of Cell Biology*, *93*(0), 438–444. https://doi.org/10.1016/j.ejcb.2014.07.003

Bernstein, L. R., & Liotta, L. A. (1994). Molecular mediators of interactions with extracellular matrix components in metastasis and angiogenesis. *Current Opinion in Oncology*, *6*(1), 106–113.

Blom, M. (2017). *The atypical Rho GTPase RhoD and its role in cellular dynamics*. Retrieved from http://openarchive.ki.se/xmlui/handle/10616/45930

Bos, J. L., Rehmann, H., & Wittinghofer, A. (2007). GEFs and GAPs: critical elements in the control of small G proteins. *Cell*, *129*(5), 865–877. https://doi.org/10.1016/j.cell.2007.05.018

Bustelo, X. R. (2000). Regulatory and signaling properties of the Vav family. *Molecular and Cellular Biology*, *20*(5), 1461–1477.

Cancer Facts & Figures 2019 | American Cancer Society. (n.d.). Retrieved March 18, 2019, from https://www.cancer.org/research/cancer-facts-statistics/all-cancer-facts-figures/cancer-facts-figures-2019.html

Chaffer, C. L., & Weinberg, R. A. (2011). A perspective on cancer cell metastasis. *Science (New York, N.Y.)*, *331*(6024), 1559–1564. https://doi.org/10.1126/science.1203543

Ching, Y.-P., Wong, C.-M., Chan, S.-F., Leung, T. H.-Y., Ng, D. C.-H., Jin, D.-Y., & Ng, I. O. (2003). Deleted in liver cancer (DLC) 2 encodes a RhoGAP protein with growth suppressor function and is underexpressed in hepatocellular carcinoma. *The Journal of Biological Chemistry*, *278*(12), 10824–10830. https://doi.org/10.1074/jbc.M208310200

Clark, E. S., Whigham, A. S., Yarbrough, W. G., & Weaver, A. M. (2007). Cortactin is an essential regulator of matrix metalloproteinase secretion and extracellular matrix degradation in invadopodia. *Cancer Research*, *67*(9), 4227–4235. https://doi.org/10.1158/0008-5472.CAN-06-3928

Condeelis, J. S., Wyckoff, J. B., Bailly, M., Pestell, R., Lawrence, D., Backer, J., & Segall, J. E. (2001). Lamellipodia in invasion. *Seminars in Cancer Biology*, *11*(2), 119–128. https://doi.org/10.1006/scbi.2000.0363

Curtius, K., Wright, N. A., & Graham, T. A. (2018). An evolutionary perspective on field cancerization. *Nature Reviews Cancer*, *18*(1), 19–32. https://doi.org/10.1038/nrc.2017.102

Delorme-Walker, V. D., Peterson, J. R., Chernoff, J., Waterman, C. M., Danuser, G., DerMardirossian, C., & Bokoch, G. M. (2011). Pak1 regulates focal adhesion strength, myosin IIA distribution, and actin dynamics to optimize cell migration. *The Journal of Cell Biology*, *193*(7), 1289–1303. https://doi.org/10.1083/jcb.201010059

Eddy, R. J., Weidmann, M. D., Sharma, V. P., & Condeelis, J. S. (2017). Tumor Cell Invadopodia: Invasive Protrusions that Orchestrate Metastasis. *Trends in Cell Biology*, *27*(8), 595–607. https://doi.org/10.1016/j.tcb.2017.03.003

El-Sibai, M., Pertz, O., Pang, H., Yip, S.-C., Lorenz, M., Symons, M., … Backer, J. M. (2008). RhoA/ROCK-mediated switching between Cdc42- and Rac1-dependent protrusion in MTLn3 carcinoma cells. *Experimental Cell Research*, *314*(7), 1540–1552. https://doi.org/10.1016/j.yexcr.2008.01.016

El-Sitt, S., Khalil, B. D., Hanna, S., El-Sabban, M., Fakhreddine, N., & El-Sibai, M. (2012). DLC2/StarD13 plays a role of a tumor suppressor in astrocytoma. *Oncology Reports*, *28*(2), 511–518. https://doi.org/10.3892/or.2012.1819

Fidyk, N., Wang, J.-B., & Cerione, R. A. (2006). Influencing cellular transformation by modulating the rates of GTP hydrolysis by Cdc42. *Biochemistry*, *45*(25), 7750–7762. https://doi.org/10.1021/bi060365h

Fortin Ensign, S. P., Mathews, I. T., Symons, M. H., Berens, M. E., & Tran, N. L. (2013). Implications of Rho GTPase Signaling in Glioma Cell Invasion and

Tumor Progression. *Frontiers in Oncology*, *3*. https://doi.org/10.3389/fonc.2013.00241

Goicoechea, S. M., Awadia, S., & Garcia-Mata, R. (2014). I'm coming to GEF you: Regulation of RhoGEFs during cell migration. *Cell Adhesion & Migration*, *8*(6), 535–549. https://doi.org/10.4161/cam.28721

Haga, R. B., & Ridley, A. J. (2016). Rho GTPases: Regulation and roles in cancer cell biology: Regulation and roles in cancer cell biology. *Small GTPases*, *7*(4), 207–221. https://doi.org/10.1080/21541248.2016.1232583

Hanahan, D. (2014). Rethinking the war on cancer. *Lancet (London, England)*, *383*(9916), 558–563. https://doi.org/10.1016/S0140-6736(13)62226-6

Hanahan, D., & Weinberg, R. A. (2000). The Hallmarks of Cancer. *Cell*, *100*(1), 57–70. https://doi.org/10.1016/S0092-8674(00)81683-9

Hanahan, D., & Weinberg, R. A. (2011). Hallmarks of Cancer: The Next Generation. *Cell*, *144*(5), 646–674. https://doi.org/10.1016/j.cell.2011.02.013

Hanna, S., & El-Sibai, M. (2013). Signaling networks of Rho GTPases in cell motility. *Cellular Signalling*, *25*(10), 1955–1961. https://doi.org/10.1016/j.cellsig.2013.04.009

Hanna, S., Khalil, B., Nasrallah, A., Saykali, B. A., Sobh, R., Nasser, S., & El-Sibai, M. (2014). StarD13 is a tumor suppressor in breast cancer that regulates cell motility and invasion. *International Journal of Oncology*, *44*(5), 1499–1511. https://doi.org/10.3892/ijo.2014.2330

Hart, M. J., Maru, Y., Leonard, D., Witte, O. N., Evans, T., & Cerione, R. A. (1992). A GDP dissociation inhibitor that serves as a GTPase inhibitor for the Ras-like protein CDC42Hs. *Science (New York, N.Y.)*, *258*(5083), 812–815.

Hill, C. S., Wynne, J., & Treisman, R. (1995). The Rho family GTPases RhoA, Rac1, and CDC42Hs regulate transcriptional activation by SRF. *Cell*, *81*(7), 1159–1170.

Hodge, R. G., & Ridley, A. J. (2016). Regulating Rho GTPases and their regulators. *Nature Reviews. Molecular Cell Biology*, *17*(8), 496–510. https://doi.org/10.1038/nrm.2016.67

Holschneider, C. H., & Berek, J. S. (2000). Ovarian cancer: Epidemiology, biology, and prognostic factors. *Seminars in Surgical Oncology*, *19*(1), 3–10. https://doi.org/10.1002/1098-2388(200007/08)19:1<3::AID-SSU2>3.0.CO;2-S

Horiuchi, A., Imai, T., Wang, C., Ohira, S., Feng, Y., Nikaido, T., & Konishi, I. (2003). Up-Regulation of Small GTPases, RhoA and RhoC, Is Associated with Tumor Progression in Ovarian Carcinoma. *Laboratory Investigation*, *83*(6), 861–870. https://doi.org/10.1097/01.LAB.0000073128.16098.31

Jay D. Hunt. (n.d.). Genetics of Cancer [LSU Health Sciences Center]. Retrieved March 18, 2019, from https://www.medschool.lsuhsc.edu/genetics_center/louisiana/article_cancer.htm

Johnson, D. I., & Pringle, J. R. (1990). Molecular characterization of CDC42, a Saccharomyces cerevisiae gene involved in the development of cell polarity. *The Journal of Cell Biology*, *111*(1), 143–152.

Ju, J. A., & Gilkes, D. M. (2018). RhoB: Team Oncogene or Team Tumor Suppressor? *Genes*, *9*(2), 67. https://doi.org/10.3390/genes9020067

Kawai, K., Seike, J., Iino, T., Kiyota, M., Iwamae, Y., Nishitani, H., & Yagisawa, H. (2009). START-GAP2/DLC2 is localized in focal adhesions via its N-terminal region. *Biochemical and Biophysical Research Communications*, *380*(4), 736–741. https://doi.org/10.1016/j.bbrc.2009.01.095

Key Statistics for Ovarian Cancer. (n.d.). Retrieved March 19, 2019, from https://www.cancer.org/cancer/ovarian-cancer/about/key-statistics.html

Khalil, B. D., Hanna, S., Saykali, B. A., El-Sitt, S., Nasrallah, A., Marston, D., … El-Sibai, M. (2014). The Regulation of RhoA at Focal Adhesions by StarD13 is Important for Astrocytoma Cell Motility. *Experimental Cell Research*, *321*(2), 109–122. https://doi.org/10.1016/j.yexcr.2013.11.023

King, H., Nicholas, N. S., & Wells, C. M. (2014). Role of p-21-activated kinases in cancer progression. *International Review of Cell and Molecular Biology*, *309*, 347–387. https://doi.org/10.1016/B978-0-12-800255-1.00007-7

Kossaï, M., Leary, A., Scoazec, J.-Y., & Genestie, C. (2018). Ovarian Cancer: A Heterogeneous Disease. *Pathobiology: Journal of Immunopathology, Molecular and Cellular Biology*, *85*(1–2), 41–49. https://doi.org/10.1159/000479006

Kurman, R. J. (2013). Origin and molecular pathogenesis of ovarian high-grade serous carcinoma. *Annals of Oncology: Official Journal of the European Society for Medical Oncology*, *24 Suppl 10*, x16-21. https://doi.org/10.1093/annonc/mdt463

Kurman, Robert J., & Shih, I.-M. (2016). The Dualistic Model of Ovarian Carcinogenesis: Revisited, Revised, and Expanded. *The American Journal of Pathology*, *186*(4), 733–747. https://doi.org/10.1016/j.ajpath.2015.11.011

Lane, J., Martin, T., Weeks, H. P., & Jiang, W. G. (2014). Structure and role of WASP and WAVE in Rho GTPase signalling in cancer. *Cancer Genomics & Proteomics*, *11*(3), 155–165.

Lauffenburger, D. A., & Horwitz, A. F. (1996). Cell migration: a physically integrated molecular process. *Cell*, *84*(3), 359–369.

Lawson, C. D., & Burridge, K. (2014). The on-off relationship of Rho and Rac during integrin-mediated adhesion and cell migration. *Small GTPases*, *5*. https://doi.org/10.4161/sgtp.27958

Lawson, C. D., & Ridley, A. J. (2018). Rho GTPase signaling complexes in cell migration and invasion. *The Journal of Cell Biology*, *217*(2), 447–457. https://doi.org/10.1083/jcb.201612069

Lengyel, E. (2010). Ovarian cancer development and metastasis. *The American Journal of Pathology*, *177*(3), 1053–1064. https://doi.org/10.2353/ajpath.2010.100105

Liao, Y.-C., & Lo, S. H. (2008). Deleted in Liver Cancer-1 (DLC-1): a tumor suppressor not just for liver. *The International Journal of Biochemistry & Cell Biology*, *40*(5), 843–847. https://doi.org/10.1016/j.biocel.2007.04.008

Liu, Y., Wang, Y., Zhang, Y., Miao, Y., Zhao, Y., Zhang, P.-X., … Wang, E.-H. (2009). Abnormal expression of p120-catenin, E-cadherin, and small GTPases is significantly associated with malignant phenotype of human lung cancer. *Lung Cancer*, *63*(3), 375–382. https://doi.org/10.1016/j.lungcan.2008.12.012

Mackay, D. J. G., & Hall, A. (1998). Rho GTPases. *Journal of Biological Chemistry*, *273*(33), 20685–20688. https://doi.org/10.1074/jbc.273.33.20685

Mandai, M., Konishi, I., Komatsu, T., Mori, T., Arao, S., Nomura, H., … Fukumoto, M. (1995). Mutation of the nm23 gene, loss of heterozygosity at the nm23 locus and K-ras mutation in ovarian carcinoma: correlation with tumour progression and nm23 gene expression. *British Journal of Cancer*, *72*(3), 691–695.

Martin, K., Reimann, A., Fritz, R. D., Ryu, H., Jeon, N. L., & Pertz, O. (2016). Spatio-temporal co-ordination of RhoA, Rac1 and Cdc42 activation during

prototypical edge protrusion and retraction dynamics. *Scientific Reports*, *6*, 21901. https://doi.org/10.1038/srep21901

Mitin, N., Roberts, P. J., Chenette, E. J., & Der, C. J. (2012). Posttranslational lipid modification of Rho family small GTPases. *Methods in Molecular Biology (Clifton, N.J.)*, *827*, 87–95. https://doi.org/10.1007/978-1-61779-442-1_6

Nasrallah, A., Saykali, B., Al Dimassi, S., Khoury, N., Hanna, S., & El-Sibai, M. (2014). Effect of StarD13 on colorectal cancer proliferation, motility and invasion. *Oncology Reports*, *31*(1), 505–515. https://doi.org/10.3892/or.2013.2861

National Cancer Institute. (2015, February 9). What Is Cancer? [CgvArticle]. Retrieved March 18, 2019, from National Cancer Institute website: https://www.cancer.gov/about-cancer/understanding/what-is-cancer

Ng, D. C.-H., Chan, S.-F., Kok, K. H., Yam, J. W. P., Ching, Y.-P., Ng, I. O.-L., & Jin, D.-Y. (2006). Mitochondrial targeting of growth suppressor protein DLC2 through the START domain. *FEBS Letters*, *580*(1), 191–198. https://doi.org/10.1016/j.febslet.2005.11.073

Olson, M. F., & Sahai, E. (2008). The actin cytoskeleton in cancer cell motility. *Clinical & Experimental Metastasis*, *26*(4), 273. https://doi.org/10.1007/s10585-008-9174-2

Ovarian Epithelial, Fallopian Tube, and Primary Peritoneal Cancer Symptoms, Tests, Prognosis, Stages [PdqCancerInfoSummary]. (2016, January 1). Retrieved March 20, 2019, from National Cancer Institute website: https://www.cancer.gov/types/ovarian/patient/about-ovarian-cancer-pdq

Perona, R., Montaner, S., Saniger, L., Sánchez-Pérez, I., Bravo, R., & Lacal, J. C. (1997). Activation of the nuclear factor-kappaB by Rho, CDC42, and Rac-1 proteins. *Genes & Development*, *11*(4), 463–475.

Pichot, C. S., Arvanitis, C., Hartig, S. M., Jensen, S. A., Bechill, J., Marzouk, S., … Corey, S. J. (2010). Cdc42-interacting protein 4 promotes breast cancer cell invasion and formation of invadopodia through activation of N-WASp. *Cancer Research*, *70*(21), 8347–8356. https://doi.org/10.1158/0008-5472.CAN-09-4149

Pollard, T. D., & Borisy, G. G. (2003). Cellular motility driven by assembly and disassembly of actin filaments. *Cell*, *112*(4), 453–465.

Qadir, M. I., Parveen, A., & Ali, M. (2015). Cdc42: Role in Cancer Management. *Chemical Biology & Drug Design*, *86*(4), 432–439. https://doi.org/10.1111/cbdd.12556

Radu, M., Semenova, G., Kosoff, R., & Chernoff, J. (2014). PAK signalling during the development and progression of cancer. *Nature Reviews Cancer*, *14*(1), 13–25. https://doi.org/10.1038/nrc3645

Raftopoulou, M., & Hall, A. (2004). Cell migration: Rho GTPases lead the way. *Developmental Biology*, *265*(1), 23–32. https://doi.org/10.1016/j.ydbio.2003.06.003

Rath, N., & Olson, M. F. (2012). Rho-associated kinases in tumorigenesis: re-considering ROCK inhibition for cancer therapy. *EMBO Reports*, *13*(10), 900–908. https://doi.org/10.1038/embor.2012.127

Ruest, P. J., Roy, S., Shi, E., Mernaugh, R. L., & Hanks, S. K. (2000). Phosphospecific antibodies reveal focal adhesion kinase activation loop phosphorylation in nascent and mature focal adhesions and requirement for the autophosphorylation site. *Cell Growth & Differentiation: The Molecular*

Biology Journal of the American Association for Cancer Research, *11*(1), 41–48.

Sahai, E., & Marshall, C. J. (2002). RHO-GTPases and cancer. *Nature Reviews. Cancer*, *2*(2), 133–142. https://doi.org/10.1038/nrc725

Sharma, V. P., Eddy, R., Entenberg, D., Kai, M., Gertler, F. B., & Condeelis, J. (2013). Tks5 and SHIP2 regulate invadopodium maturation, but not initiation, in breast carcinoma cells. *Current Biology: CB*, *23*(21), 2079–2089. https://doi.org/10.1016/j.cub.2013.08.044

Siegel, R. L., Miller, K. D., & Jemal, A. (2019). Cancer statistics, 2019. *CA: A Cancer Journal for Clinicians*, *69*(1), 7–34. https://doi.org/10.3322/caac.21551

Soccio, R. E., & Breslow, J. L. (2003). StAR-related lipid transfer (START) proteins: mediators of intracellular lipid metabolism. *The Journal of Biological Chemistry*, *278*(25), 22183–22186. https://doi.org/10.1074/jbc.R300003200

Spagnoli, F. M., & Brivanlou, A. H. (2006). The RNA-binding protein, Vg1RBP, is required for pancreatic fate specification. *Developmental Biology*, *292*(2), 442–456.

Stengel, K., & Zheng, Y. (2011). Cdc42 in oncogenic transformation, invasion, and tumorigenesis. *Cellular Signalling*, *23*(9), 1415–1423. https://doi.org/10.1016/j.cellsig.2011.04.001

Takai, Y., Sasaki, T., & Matozaki, T. (2001). Small GTP-binding proteins. *Physiological Reviews*, *81*(1), 153–208. https://doi.org/10.1152/physrev.2001.81.1.153

Tarin, D. (2011). Cell and tissue interactions in carcinogenesis and metastasis and their clinical significance. *Seminars in Cancer Biology*, *21*(2), 72–82. https://doi.org/10.1016/j.semcancer.2010.12.006

Thiery, J. P. (2002). Epithelial-mesenchymal transitions in tumour progression. *Nature Reviews. Cancer*, *2*(6), 442–454. https://doi.org/10.1038/nrc822

Thorsell, A.-G., Lee, W. H., Persson, C., Siponen, M. I., Nilsson, M., Busam, R. D., … Lehtiö, L. (2011). Comparative structural analysis of lipid binding START domains. *PloS One*, *6*(6), e19521. https://doi.org/10.1371/journal.pone.0019521

Tomar, A., Lim, S.-T., Lim, Y., & Schlaepfer, D. D. (2009). A FAK-p120RasGAP-p190RhoGAP complex regulates polarity in migrating cells. *Journal of Cell Science*, *122*(Pt 11), 1852–1862. https://doi.org/10.1242/jcs.046870

Torre, L. A., Trabert, B., DeSantis, C. E., Miller, K. D., Samimi, G., Runowicz, C. D., … Siegel, R. L. (2018). Ovarian cancer statistics, 2018. *CA: A Cancer Journal for Clinicians*, *68*(4), 284–296. https://doi.org/10.3322/caac.21456

Tucci, M. G., Lucarini, G., Brancorsini, D., Zizzi, A., Pugnaloni, A., Giacchetti, A., … Biagini, G. (2007). Involvement of E-cadherin, beta-catenin, Cdc42 and CXCR4 in the progression and prognosis of cutaneous melanoma. *The British Journal of Dermatology*, *157*(6), 1212–1216. https://doi.org/10.1111/j.1365-2133.2007.08246.x

Types & Stages - National Ovarian Cancer Coalition. (n.d.). Retrieved March 19, 2019, from http://ovarian.org/about-ovarian-cancer/what-is-ovarian-cancer/types-a-stages

Van Aelst, L., & D'Souza-Schorey, C. (1997). Rho GTPases and signaling networks. *Genes & Development*, *11*(18), 2295–2322.

Verkhovsky, A. B., Svitkina, T. M., & Borisy, G. G. (1999). Self-polarization and directional motility of cytoplasm. *Current Biology: CB*, *9*(1), 11–20.

What Is Ovarian Cancer? (2019). Retrieved March 19, 2019, from https://www.cancer.org/cancer/ovarian-cancer/about/what-is-ovarian-cancer.html

Yamaguchi, H. (2012). Pathological roles of invadopodia in cancer invasion and metastasis. *European Journal of Cell Biology*, *91*(11–12), 902–907. https://doi.org/10.1016/j.ejcb.2012.04.005

Yamaguchi, Hideki, Lorenz, M., Kempiak, S., Sarmiento, C., Coniglio, S., Symons, M., … Condeelis, J. (2005). Molecular mechanisms of invadopodium formation: the role of the N-WASP-Arp2/3 complex pathway and cofilin. *The Journal of Cell Biology*, *168*(3), 441–452. https://doi.org/10.1083/jcb.200407076

Yang, N., Higuchi, O., Ohashi, K., Nagata, K., Wada, A., Kangawa, K., … Mizuno, K. (1998). Cofilin phosphorylation by LIM-kinase 1 and its role in Rac-mediated actin reorganization. *Nature*, *393*(6687), 809–812. https://doi.org/10.1038/31735

Zhan, Y., Abi Saab, W. F., Modi, N., Stewart, A. M., Liu, J., & Chadee, D. N. (2012). Mixed Lineage Kinase 3 is Required for Matrix Metalloproteinase Expression and Invasion in Ovarian Cancer Cells. *Experimental Cell Research*, *318*(14), 1641–1648. https://doi.org/10.1016/j.yexcr.2012.05.002

Zhou, F.-Q., & Snider, W. D. (2006). Intracellular control of developmental and regenerative axon growth. *Philosophical Transactions of the Royal Society of London B: Biological Sciences*, *361*(1473), 1575–1592. https://doi.org/10.1098/rstb.2006.1882